Ecological Indicators 190 (2026) 115283

Contents lists available at ScienceDirect

Ecological Indicators

journal homepage: www.elsevier.com/locate/ecolind

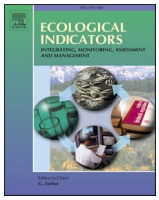

# Drone-measured canopy spectra can be a complementary predictor of belowground arbuscular mycorrhizal fungi variations in urban community gardens

Yasamin Afrasiabian [a], Diana Rocío Andrade-Linares [b,e], Stefanie Schulz [b], Michael Schloter [b], Elisa Van Cleemput [c], Monika Egerer [d], Kang Yu [a,*]

[a] Precision Agriculture Lab, TUM School of Life Sciences, Technical University of Munich, Dürnast 9, 85354 Freising, Germany
[b] Research Unit Comparative Microbiome Analysis, Helmholtz Zentrum München, Ingolstaedter Landstraße 1, D-85764 Neuherberg, Germany
[c] Leiden University College The Hague, Leiden University, Anna van Buerenplein 301, 2595, DG, Den Haag, the Netherlands
[d] Urban Productive Ecosystems, TUM School of Life Sciences, Technical University of Munich, Hans Carl-von-Carlowitz-Platz 2, 85354 Freising, Germany
[e] Research Group of Environmental Microbiology, Biological Sciences Department, University of Limerick, Limerick V94 T9PX, Ireland

ARTICLE INFO

*Keywords:*
Below-ground biodiversity
UAV multispectral remote sensing
Urban community gardens
Canopy ecological indicator
Piecewise SEM
Vegetation indices
GLCM texture

ABSTRACT

Arbuscular mycorrhizal fungi (AMF) form essential symbioses with plant roots, improving nutrient uptake, plant health, and soil function. However, assessing AMF abundance in urban ecosystems remains challenging. Drone-based multispectral imaging can estimate canopy functional traits, raising the question of whether variation in aboveground canopy metrics can serve as an ecological indicator of belowground AMF abundance. We sampled five community gardens over two growing seasons, combining quadrat-level plant surveys, soil sampling for AMF abundance, Unmanned Aerial Vehicle (UAV) multispectral imagery, and point clouds. From the UAV, we derived vegetation indices, spectral diversity and texture metrics, and from the point clouds we extracted canopy height metrics. We related these traits to log AMF abundance using LASSO cross-validated regression and piecewise structural equation modelling (SEM). Our analyses showed that drone-derived canopy traits captured part of the aboveground variation associated with belowground AMF abundance, particularly through canopy greenness and image texture patterns. Higher AMF abundance was associated with greener and more vertically heterogeneous canopies. UAV-derived canopy texture features explained up to ~38% of the variance in AMF abundance. Piecewise SEM indicated that AMF abundance was associated with a non-linear climate response, represented by the quadratic climate term ($\beta = 0.25$) and a positive vegetation-index pathway ($\beta = 0.21$). The AMF abundance SEM model had a marginal $R^2$ of 0.62, suggesting that seasonal climatic conditions and canopy greenness jointly structured AMF variation. Overall, UAV-derived canopy traits represent a scalable ecological indicator of relative AMF abundance in urban gardens, supporting non-destructive assessment of relative AMF variation and spatial targeting of field sampling. Establishing this link provides a baseline for developing stronger urban ecological indicators by integrating UAV data with soil measurements, garden management, and higher-resolution remote-sensing approaches.

## 1. Introduction

Monitoring biodiversity from aboveground to belowground, and understanding its consequences for ecosystem functioning, are critical challenges under rapid global change and accelerating urbanisation. The interactions between aboveground plant communities and belowground microbial communities are complex and characterized by reciprocal influences among plants and microbes (De Deyn and Van Der Putten, 2005; Forero et al., 2021; Kardol and Wardle, 2010). The organic inputs provided by plants fuel microbial activity (Egidi et al., 2025; Guo et al., 2023; Lange et al., 2015a; Schmid et al., 2021), while soil microorganisms enhance nutrient availability and thereby influence plant health and diversity (Igiehon and Babalola, 2018; Soudzilovskaia et al., 2019; Van Der Heijden et al., 1998). One of the most important adaptations of terrestrial plants is mycorrhizal symbiosis, partnerships between plant roots and fungi (Soudzilovskaia et al., 2020). In these

* Corresponding author at: TUM Precision Agriculture Lab, Dürnast 9, 85354 Freising, Germany.
*E-mail address:* kang.yu@tum.de (K. Yu).

https://doi.org/10.1016/j.ecolind.2026.115283
Received 8 April 2026; Received in revised form 29 June 2026; Accepted 26 July 2026
Available online 4 August 2026

relationships, plants provide photosynthate sugars, while fungal partners enhance water and nutrient uptake and help protect plants against biotic and abiotic stresses (Bell et al., 2024). Among recognised mycorrhizal types, arbuscular mycorrhizal fungi (AMF) are pivotal symbionts that associate with roughly 72% of vascular plant species (Brundrett and Tedersoo, 2018; Wang et al., 2023). The symbiosis between AMF and host plant roots facilitates greater nutrient absorption, particularly for essential elements such as phosphorus (P) and nitrogen (N) (Helber et al., 2011). AMF improve nutrient uptake by extending the root surface area through their hyphal networks, which reach beyond the immediate root zone to access soil nutrients that are often immobile or unavailable in the inter-root zone (Helber et al., 2011; Sun et al., 2018). By altering plant nutrient and water status in this way, AMF can influence leaf chemistry, growth and canopy architecture, and thus the biochemical, biophysical and structural traits of plant canopies.

Assessing and quantifying AMF interactions poses significant challenges, particularly in urban environments characterized by heterogeneous soil conditions, diverse management practices, and multiple stressors. Traditional methods for measuring AMF abundance and colonization, such as root staining and microscopy, quantitative PCR and metabarcoding, are often destructive, labour-intensive, and poorly suited for large-scale or repeated monitoring in dynamic urban ecosystems (Jiang et al., 2020; Scheublin et al., 2004). Given the important role of AMF in sustaining plant and soil health, nutrient cycling, and ecosystem resilience, there is an urgent need for non-invasive approaches to evaluate their abundance and functional impacts.

Remote sensing, especially imaging spectroscopy, reliably assesses aboveground biodiversity and crop health by mapping canopy biophysical traits (physical structure and structural characteristics) and biochemical traits (chemical composition, metabolic activities and internal processes) that reveal vegetation function and structure (Afrasiabian et al., 2025; Cavender-Bares et al., 2021; Van Cleemput et al., 2018; Wang and Gamon, 2019). For example, RGB and multispectral imaging detect proxies of chlorophyll and water status (e.g. vegetation indices), structural attributes (e.g. canopy height), and heterogeneity metrics (texture and spectral diversity), offering a non-destructive way to assess biodiversity and ecosystem functioning (Li et al., 2025; Ludwig et al., 2024; Rossi and Gholizadeh, 2023; Taddeo et al., 2021). Remote sensing of aboveground canopy traits has advanced significantly, particularly through the application of satellite and Unmanned Aerial Vehicle (UAV) imaging spectroscopy. Vegetation canopy reflectance and absorption arise from interacting structural, biochemical, physiological and phenological traits, which imaging spectroscopy can measure non-destructively across space and time. These advances demonstrate that canopy spectra integrate information on leaf chemistry and structure, including pigments, water content, leaf area index and architecture, enabling assessments of plant function at community scales where belowground processes are shaped by the quantity and quality of plant inputs. As a result, remotely sensed canopy traits are increasingly used as integrative indicators of ecosystem functioning (Cavender-Bares et al., 2022; Schweiger et al., 2018; Wang and Gamon, 2019).

Extending this approach to link canopy characteristics with belowground symbionts such as AMF offers a promising, non-destructive way to infer spatial variation in root-fungus associations, particularly in structurally complex ecosystems. This link is plausible because canopy spectral and structural traits can reflect plant physiological status, cover, and spatial heterogeneity, all of which may be influenced by belowground interactions between plants and soil microorganisms. However, unlike aboveground vegetation properties that can be directly measured from imagery, remotely detecting belowground processes remains technically difficult and poorly resolved. AMF therefore cannot be observed directly by UAV imagery; instead, canopy traits can serve as indirect indicators of how the effects of belowground symbioses are reflected in aboveground plant parts. Although theory and emerging evidence suggest that canopy health, complexity, and heterogeneity should co-vary with belowground AMF (Stahlhut et al., 2024), it remains unclear how well and which remotely sensed aboveground plant traits can explain spatial variation in microbial abundance at ecologically relevant scales. Only a few studies suggest that remotely sensed canopy traits may help overcome some limitations of traditional assessment techniques for belowground biodiversity (Fisher et al., 2016; Sousa et al., 2021).

So far, remote sensing-microbe studies have generally followed two main directions: using canopy spectra to characterize habitat or plant functional traits associated with soil microbial communities, and using imaging spectroscopy to predict broad microbial groups or community composition across larger grassland, forest or multi-biome datasets (Cavender-Bares et al., 2022; Harris and Bardgett, 2025). This leaves AMF abundance less well resolved, particularly in urban community gardens where canopy composition, soil conditions and management vary at much finer spatial scales than in most grassland, forest or continental-scale studies. Therefore, beyond the question of whether canopy reflectance can be related to soil microbes in general, it remains unclear which UAV-derived canopy traits can indicate AMF-specific abundance in fine-scale, heterogeneous urban vegetation. Moreover, previous studies have used canopy spectral reflectance as the main predictor (for example, airborne or satellite imaging spectroscopy), whereas the complementary information in other UAV imagery-derived features, namely spectral diversity, spatial texture, and canopy structural (height) metrics of the ground vegetation, has rarely been tested as an indicator of belowground AMF abundance. The effectiveness of using canopy traits as ecological indicators of AMF abundance in urban ecosystems, however, remains mostly unexplored. Key questions remain regarding the generality of canopy-AMF links across different ecological contexts and scales. For instance, can variations in canopy structure be reliably correlated with AMF abundance across diverse plant communities and urban landscapes? Moreover, the integration of remote sensing data with traditional mycorrhizal assessment methods could provide richer insights into AMF interactions with urban plant communities, thus facilitating better management practices for urban ecology.

Urban gardens are one example of structurally complex and dynamic ecosystems over space and time that are challenging to measure using meaningful ecological indicators. Urban community gardens are small, highly managed green spaces embedded in dense urban areas, and they often contain a patchwork of beds, paths, and mixed wild and cultivated vegetation (Sexton et al., 2025a, 2025b). This fine-scale heterogeneity creates strong variation in canopy structure and soil conditions over short distances and across the growing season, which makes it difficult to track biodiversity and ecosystem functioning with standard field indicators alone. This makes urban gardens an ecologically distinct test system, because canopy composition, management disturbance and soil conditions develop and vary differently from conventional vegetation systems. Scalable indicators that link aboveground canopy properties to belowground processes could therefore be especially useful in gardens, where monitoring needs to be repeatable and non-destructive. The key spatial challenge is whether variation among neighbouring plant assemblages can reveal relative differences in belowground AMF abundance in managed, heterogeneous urban community garden vegetation systems.

Based on this rationale, we hypothesised that higher variations of chlorophyll-related vegetation indices, greater canopy structural complexity, and greater plant community diversity would be associated with higher AMF abundance (Fig. 1). We also expected that metrics of local canopy variation, such as spectral diversity and texture features, would improve predictions of AMF abundance beyond greenness measures alone. To test these assumptions, we investigate the question: Can drone-based canopy spectral features predict belowground AMF abundance, and thus provide a non-invasive way to measure plant-AMF relationships? In particular, we (i) examine spatial and temporal patterns in AMF abundance in urban community gardens and their relationships

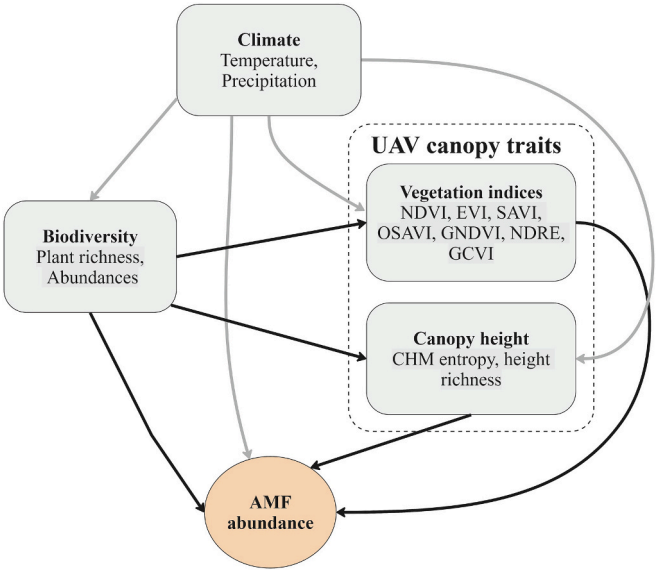


**Fig. 1.** A priori piecewise structural equation model (SEM) showing hypothesised direct and indirect pathways linking climate (temperature and precipitation), biodiversity (richness and abundance), UAV-derived canopy traits (vegetation indices and canopy height metrics), and AMF abundance (log10). Black arrows indicate hypothesised positive effects and grey arrows indicate tested effects for which no directional hypothesis was specified.

with climate and local biodiversity; (ii) quantify how well different UAV canopy-trait groups (spectral diversity, vegetation indices, image texture and canopy-height metrics) explain quadrat-scale variation in AMF using cross-validated machine-learning models; and (iii) use piecewise structural equation modelling (SEM) to test direct and indirect pathways through which climate, biodiversity and canopy traits jointly influence AMF abundance.

## 2. Materials and methods

### 2.1. Study area and sampling design

The study was conducted in five urban community gardens within the city of Munich, Germany: Essbare Stadt (ESS), Freihamer Freiluftgarten (FF), Karlsfeld Community Garden (KF), StadtAcker (SA), and Sonnengarten Solln (SONN) (Fig. 2, Table 1). Data collection spanned 2021 and 2022, with sampling conducted three times per year. In 2021, sampling occurred in July, August, and October; in 2022, it took place in May, July, and October. To standardize sampling, a 20 × 20 m plot was established in the central area of each garden during each round. Within each plot, eight 1 × 1 m quadrats were randomly positioned for data collection (Fig. 2b). Plots and quadrats were relocated between sampling rounds and years, with no permanent markers used; therefore, the quadrats were treated as plot-level observations within a garden rather than as repeated measurements of identical permanent quadrats. Garden identity was included as a grouping factor in the statistical analyses to account for shared spatial context and management conditions among quadrats. This design yielded 40 quadrats per round (5 gardens × 8 quadrats), approximately 120 quadrats per year, and a total of 240 quadrats across the study (Table 1). Precise geolocation of each plot was achieved using Real-Time Kinematic (RTK) GPS.

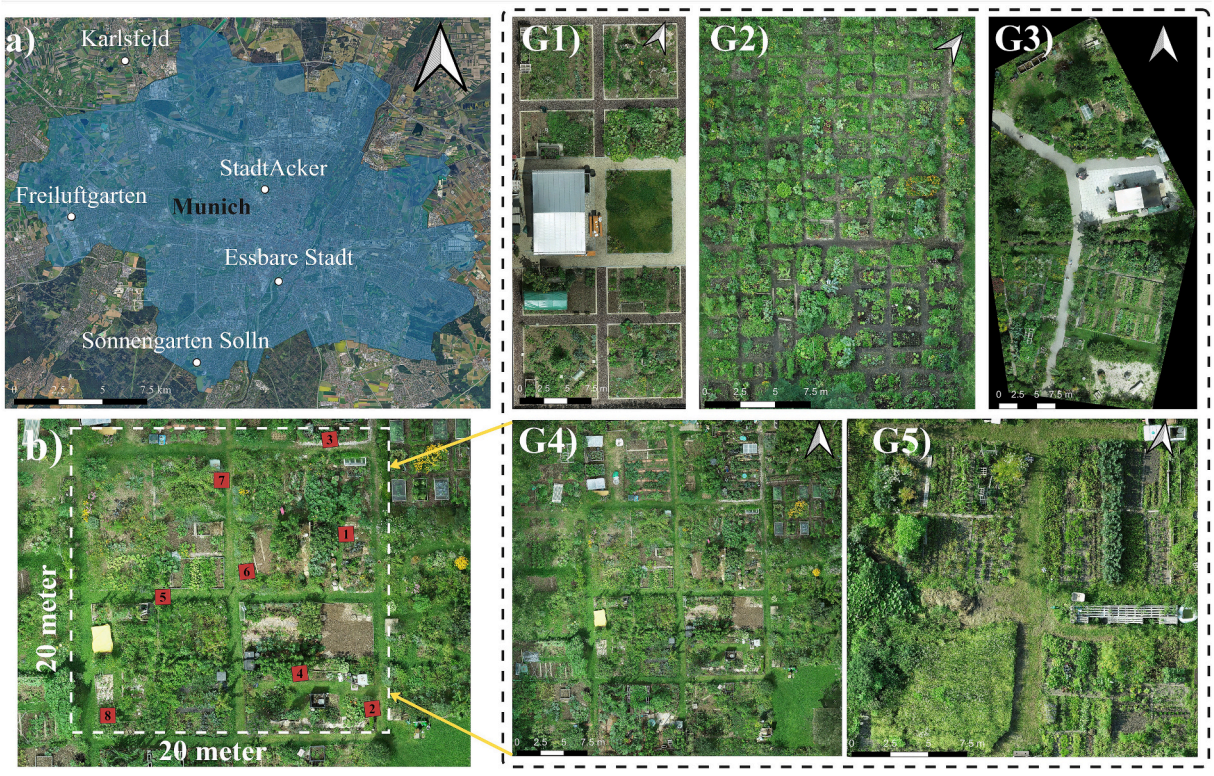


**Fig. 2.** (a) Location of the five community gardens within the urban extent of Munich. (b) Example UAV RGB orthomosaic of one garden showing the 20 × 20 m sampling plot (white dashed square) and the eight 1 × 1 m quadrats (red squares, numbered 1–8) used for paired canopy and belowground sampling. (G1–G5) UAV orthomosaics of the five community gardens: Freiluftgarten Freiham (G1), Essbare Stadt (G2), StadtAcker (G3), Sonnengarten Solln (G4), and Karlsfeld Community Garden (G5), illustrating variation in garden layout, vegetation structure, and management across sites. (For interpretation of the references to colour in this figure legend, the reader is referred to the web version of this article.)

**Table 1**
Summary of the five urban community gardens in Munich, including garden area in square meters ($m^2$), mean elevation (m), percentage of built-up area within a 1 km buffer, year established, and main use. Garden boundaries were digitized based on UAV-derived images, and built-up area estimates were derived from the ESA WorldCover 10 m land cover product (version 2.0, year 2021).

| Garden | Area ($m^2$) | Mean Elevation (m) | Built-up Area (%) | Established (Year) | Main Use |
|---|---|---|---|---|---|
| ESS | 575.1 | 563.82 | 55.31 | 2010 | Gardening; demonstration garden |
| FF | 778.1 | 573.71 | 33.91 | 2020 | Organic gardening; biodiversity; sustainability workshops |
| KF | 519.5 | 533.14 | 9.08 | 2015 | Organic gardening; biodiversity; social space |
| SA | 1065.5 | 560.28 | 52.06 | 2017 | Organic gardening; biodiversity; community activities |
| SONN | 1280.6 | 614.55 | 26.48 | 2014 | Organic gardening; biodiversity; community collaboration |

### 2.2. Biodiversity and plant community variables

Within each 1 × 1 m quadrat, we conducted detailed vegetation surveys during every sampling campaign. All vascular plant species rooted within the quadrat were identified to the lowest possible taxonomic level in the field, and their abundance was recorded using a standardized visual estimation protocol. Plant surveys were carried out on the same dates and within the same quadrats as soil sampling, and within 1–2 days interval of the UAV acquisitions, ensuring spatial and temporal correspondence between aboveground vegetation, belowground AMF measurements, and canopy traits.

In this study, we derived two biodiversity metrics from the survey data. Plant species richness was defined as the number of distinct plant species recorded per quadrat. Total plant abundance was calculated as the sum of the abundance values of all species present in each quadrat, providing an integrative measure of stand density and overall vegetation development.

In addition to these two biodiversity metrics used in the main SEM framework, we used the full plant species-cover table to explicitly include vegetation identity in response to the importance of host-plant context for AMF. Each quadrat was classified into one of six community types: Bare/low vegetation cover, Grass, Herb, Crop/vegetable, Legume, and Mixed high-diversity. Classification was based on field survey data, including plant species identity, species cover, ground-cover type, species richness, and Shannon diversity. Bare/low vegetation quadrats were defined by low plant species cover ($< 20\%$) and low live vegetation cover ($< 30\%$), or by very low richness ($\leq 1$ species). Grass, Crop/vegetable, Legume, and Herb types were assigned when the corresponding functional group dominated species cover or field cover ($\geq 30\%$ grass field cover, $\geq 25\%$ crop/vegetable cover, $\geq 15\%$ legume cover, or $\geq 25\%$ herb cover). Mixed high-diversity quadrats were defined as species-rich or Shannon-diverse quadrats ($\geq 6$ species or Shannon diversity above the 75th percentile) without dominance by a single functional group ($< 55\%$ of total species cover). To test whether community type was associated with AMF abundance, log AMF abundance was modelled using a linear model with community type as the main predictor and garden identity and sampling month as covariates (Fig. 8). To further examine whether individual plant species were associated with AMF abundance, we performed a species-level cover analysis (Table S5). Only species recorded in at least eight quadrats were included, because very rare species provide unstable statistical estimates. For each species, we fitted a separate linear model in which log AMF abundance was the response variable and the cover of that species was the main predictor. Garden identity and sampling month were included as covariates to account for spatial and temporal variation. Species cover was scaled so that the model coefficient represented the expected change in log AMF abundance for each 10% increase in cover of that species. Because many species were tested, *p*-values were adjusted using the Benjamini-Hochberg false-discovery-rate procedure.

After extracting UAV vegetation indices and GLCM texture features (Supplementary Methods S1), we tested whether these metrics differed among the field-defined community types using PCA ordination and PERMANOVA (Fig. S3). This analysis evaluated the extent to which UAV-derived greenness and texture reflected the field-observed vegetation differences relevant to AMF. We did not classify plant species or community types from the imagery; community types were defined solely from the field survey, and the UAV metrics were compared among these groups. Climate data.

To characterize the climatic context during our study, we used variables from the ERA5-Land reanalysis product, which provides long-term, high-resolution estimates of land-surface conditions (Copernicus Climate Change Service, 2019; Muñoz-Sabater et al., 2021). We extracted monthly precipitation (in mm) and near-surface air temperature (in °C) for the grid cell covering the Munich metropolitan area during 2021 and 2022, aligning with our vegetation, soil, and UAV data collection in the urban gardens. For each month in those years, we gathered total precipitation and mean air temperature, using these time series to highlight inter-annual and seasonal variations in climate conditions and to situate our sampling campaigns within Munich's broader hydroclimatic patterns. Since the five community gardens span a relatively compact urban area, we assumed the ERA5-Land grid cell for Munich effectively captured the large-scale climate shared across all sites. These climate variables helped describe growing-season dynamics and interpret trends in canopy traits and AMF abundance.

### 2.3. Soil sampling and AMF quantification by quantitative polymerase chain reaction (qPCR)

To quantify belowground AMF at the same spatial scale as the vegetation surveys, we collected soil samples within each 1 × 1 m quadrat. In every quadrat, we obtained five soil cores from the upper 0–30 cm of the soil using an auger: one from each corner and one from the centre. We removed coarse roots, stones, and visible organic debris in the field, then combined the subsamples into a single composite sample representing the quadrat-level topsoil. We gently homogenized the composites, passed them through a 2 mm sieve to standardize particle size and remove remaining coarse material, and immediately transferred subsamples for AMF analyses into sterile tubes. These were flash-frozen in liquid nitrogen and stored at ultra-low temperature in the field, and then transferred to a − 30 °C freezer. We transported samples to the analytical laboratory on dry ice to preserve DNA integrity and microbial signals, yielding one soil sample, and thus one AMF abundance estimate, per quadrat.

AMF abundance was quantified using a DNA-based approach. Total genomic DNA was extracted from 500 mg of homogenized soil as described previously by Andrade-Linares et al. (2023). DNA concentration (ng $\mu L^{-1}$), soil fresh weight, and soil dry weight were determined for each sample. Aliquots of the DNA extracts were then diluted (1:64) and analysed by qPCR, targeting the large subunit of the rRNA gene of AMF. Abundance of AMF was assessed by using 0.5 pmol µl − 1 of primers FLR3 and FLR4, which target AMF species belonging to the families *Glomeraceae, Gigasporaceae, Archaeosporaceae and Acaulosporaceae* (Gollotte et al., 2004; Mummey and Rillig, 2007). qPCR conditions and primers are described by Andrade-Linares et al. (2023). All qPCR calibration curves showed efficiencies were higher than 80% with

coefficient of determination ($R^2$) of the standard curves above 0.99. The specificity of the amplified products was checked by melting curves of the amplicons and on 2% agarose gels. The AMF gene copy numbers were calculated per gram of soil dry weight by combining information on the soil fresh-to-dry mass ratio (DW/FW), the total DNA extraction elution volume, the applied dilution factor, and the qPCR-derived quantity per reaction based on a standard curve. The resulting values, expressed as AMF gene copies $g^{-1}$ dry soil, were used as the measure of AMF abundance for all statistical analyses.

### 2.4. UAV image acquisition and canopy trait extraction

We acquired canopy-level spectral and structural data using a Phantom 4 Multispectral and RGB RTK UAV (DJI, Shenzhen, China). To ensure close temporal alignment between remotely sensed canopy traits and in-situ vegetation and soil measurements, we conducted flights within 1–3 days of the field campaigns, accounting for local climate and airspace constraints. We adjusted flight altitudes based on garden-specific canopy heights, achieving ground resolution of approximately 13 mm $pixel^{-1}$ at 25 m (ESS, SA), 11 mm $pixel^{-1}$ at 20 m (SONN), and 8 mm $pixel^{-1}$ at 15 m (FF, KF).

We performed image preprocessing and 3D reconstruction in Agisoft Metashape (version 1.8.4). The RTK (Real-Time Kinematic) corrections system using SAPOS (Bavaria) provided centimeter-level georeferencing accuracy without the use of ground control points (GCPs) during image acquisition. Using a structure-from-motion workflow with high overlap (approximately 90% front and side), we aligned the raw multispectral and RGB images and georeferenced the resulting sparse point clouds in the ETRS89 / UTM zone 32 N coordinate system via RTK metadata. We then generated dense point clouds to derive high-resolution digital surface models (DSM). Where required, we created digital terrain models (DTM) and subtracted them from DSMs to produce canopy height models (CHMs). To minimize illumination variations, we applied Metashape's radiometric normalization procedures. Finally, we exported band-aligned, georeferenced orthomosaics at garden-specific resolutions (8–13 mm $pixel^{-1}$). These orthomosaics and CHMs served as the foundation for calculating quadrat-scale canopy spectral, structural, and texture metrics.

From the multispectral orthomosaics and CHMs, we extracted quadrat-level canopy metrics describing canopy condition, heterogeneity, texture, and vertical structure. Metrics included (i) spectral diversity, (ii) vegetation indices, (iii) texture features, and (iv) CHM-derived structural variables. These metrics were used as indicators of AMF abundance. An overview of all canopy metrics and their references is provided in Table 2. Full definitions, parameter settings, and computational details are provided in Supplementary Methods S1 and Supplementary Table S1.

### 2.5. Principal component analysis and bivariate relationships

To summarize sets of correlated indicators into single composite axes, we applied principal component analysis (PCA) to standardized variables. Analyses were conducted in Python (version 3.12.4) using scikit-learn (version 1.7.0) for standardization and PCA. PCA was performed on z-standardized variables using standard singular value decomposition. Monthly climate conditions were reduced by running PCA on mean air temperature and total monthly precipitation from ERA5-Land across all sampling months; the PC1 was used as the climatic indicator in subsequent analyses. Biodiversity was similarly summarised by applying PCA to quadrat-level plant species richness and total plant abundance, as a composite diversity axis.

For UAV data, we conducted separate PCAs for each canopy metric group: (i) spectral diversity metrics, (ii) texture features, (iii) vegetation indices and (iv) canopy-height metrics. Within each group, PC1 represented the main gradient in that trait family and was used as a composite indicator. Relationships between log AMF abundance and individual UAV metrics, as well as between AMF and the group-specific PC1 scores, were quantified using Pearson correlation and simple linear regression. We report correlation coefficients (r) and *p*-values in the Results.

**Table 2**
Overview of canopy metrics derived from UAV multispectral imagery and canopy height models (CHMs) used as indicators of arbuscular mycorrhizal fungi (AMF) abundance. Metrics are grouped into spectral diversity measures, vegetation indices, grey-level co-occurrence matrix (GLCM) texture features, and CHM-derived structural variables.

| Category | Metric name | Symbol | Reference |
|---|---|---|---|
| Spectral Diversity | Coefficient of variation | CV | (Wang et al., 2016) |
| | Spectral entropy | $H_{spec}$ | (Shannon, 1948) |
| | Spectral angle mapper | $\theta_{SAM}$ | (Kruse et al., 1993) |
| Vegetation Indices | Normalized Difference Vegetation Index | NDVI | (Rouse et al., 1974) |
| | Green NDVI | GNDVI | (Gitelson et al., 1996) |
| | Normalized Difference Red Edge | NDRE | (Gitelson and Merzlyak, 1994) |
| | Enhanced Vegetation Index | EVI | (Huete et al., 2002) |
| | Soil-Adjusted Vegetation Index | SAVI | (Huete, 1988) |
| | Optimized SAVI | OSAVI | (Rondeaux et al., 1996) |
| | Green Chlorophyll Vegetation Index | GCVI | (Gitelson et al., 2003) |
| Texture Features (GLCM) | Contrast | CON | (Haralick et al., 1973) |
| | Correlation | COR | (Haralick et al., 1973) |
| | Energy | ENG | (Haralick et al., 1973) |
| | Homogeneity | HOM | (Haralick et al., 1973) |
| Canopy Height Metrics | Height entropy | $H_h$ | (Valbuena et al., 2012) |
| | Structural richness | $S_h$ | (McElhinny et al., 2005) |

### 2.6. Machine learning modelling and analysis

Our primary objective was to quantify how well drone-derived canopy traits predict spatial variation in AMF abundance at the quadrat scale. All analyses were conducted with log AMF abundance as the response variable and standardized predictors (canopy traits, biodiversity metrics and, where specified, climate covariates), as described above. Quadrats with missing values for AMF or any of the canopy predictors were excluded from the analysis to avoid imputation and preserve the integrity of measured relationships.

We modelled the relationship between UAV canopy traits and AMF abundance using penalized linear regression with embedded feature selection. For each canopy trait family (spectral diversity, texture, vegetation indices, canopy height), we assembled all available UAV-derived predictors and used log AMF abundance as the response. Feature selection and modelling were implemented jointly through the least absolute shrinkage and selection operator (LASSO) in a linear regression model (Tibshirani, 1996). Predictors were standardized before model fitting so that the LASSO penalty operated on a common scale across traits. To avoid imposing an arbitrary limit on model complexity, the optimal number of retained LASSO-ranked predictors was tuned separately for each UAV metric group using nested cross-validation. The dataset was divided into up to ten outer folds, with each fold used once as an independent test dataset. Within every outer training dataset, an additional five-fold inner cross-validation evaluated all possible maximum numbers of retained LASSO-ranked predictors, ranging from one predictor to the total number available within the respective predictor group. The predictor-count limit minimizing inner-cross-validation root mean squared error (RMSE) was selected and used

to fit the linear-regression model, which was subsequently evaluated on the untouched outer test fold. Thus, neither predictor selection nor selection of the number of retained predictors used information from the corresponding outer test fold. Because the optimal predictor count was independently selected within every outer training fold, the selected number could differ among folds and predictor groups. The median and range of selected predictor counts were used to summarize model complexity. For descriptive comparison, we additionally examined outer-cross-validation RMSE across fixed predictor-count limits (Fig. S1).

Model fitting and feature selection were evaluated using K-fold cross-validation with up to 10 folds. For a given trait family, the dataset was first restricted to rows with complete observations for all predictors in that family and the AMF response, and then randomly partitioned into K folds (with $K \leq 10$, adjusted when the sample size was small). For each outer fold, a modelling pipeline was refitted from scratch on the remaining K-1 folds: predictors were standardized, a LASSO model with its penalty parameter tuned by internal cross-validation was estimated on the training data, and the resulting set of non-zero-coefficient predictors was passed to an ordinary least-squares linear regression model. This pipeline was then used to predict AMF abundance in the held-out fold, yielding out-of-fold predictions for all samples. By rerunning feature selection and penalty tuning separately inside each outer fold, this procedure follows established recommendations that all steps of model building, including variable selection, be nested within cross-validation to avoid optimistic bias in estimated prediction error.

Predictive performance for each trait family was summarised using the coefficient of determination ($R^2$), computed as the squared Pearson correlation between observed and out-of-fold predicted AMF values, and RMSE of the same predictions. These metrics quantify, respectively, the proportion of variance in AMF abundance explained under cross-validation and the typical prediction error on the log-scale. After cross-validation, we refitted the LASSO–linear regression pipeline on the full dataset for each trait family using the same procedure, and extracted the standardized regression coefficients of the retained predictors. These coefficients provide an interpretable measure of the direction and relative strength of association between each selected UAV canopy metric and AMF abundance, conditional on the other predictors in the model. In addition, we assessed the robustness of the UAV prediction models using 100 iterations of random 80:20 train-test splitting. Within each iteration, the complete nested modelling pipeline, including predictor standardization, LASSO feature selection, and linear-regression fitting, was refitted using only the training data and evaluated on the held-out test data. Model performance was summarised using the squared Pearson correlation between observed and predicted log AMF abundance ($R^2$) and root mean squared error (RMSE; Table S2).

### 2.7. Piecewise structural equation modelling (SEM)

We applied a piecewise structural equation modelling (SEM) framework to assess how climate, local biodiversity, and UAV-derived canopy traits collectively influence AMF abundance. SEM is well suited for this purpose because it allows several linked hypotheses to be evaluated simultaneously, and separates direct effects from indirect effects that operate through intermediate variables, rather than relying on a single, straightforward regression (Lefcheck, 2016). The piecewise approach, which breaks the model into linked components, was particularly suitable for our hierarchically structured data (quadrats within gardens) and allowed us to incorporate mixed-effects regressions where needed.

The hypothesised causal network (Fig. 7) consisted of four linked linear mixed-effects models: (i) biodiversity as a function of climate; (ii) vegetation indices as a function of climate and biodiversity; (iii) canopy height as a function of climate and biodiversity; and (iv) AMF abundance as a function of climate (PC1 and quadratic term $PC1^2$), biodiversity, vegetation indices and canopy height. We included the quadratic climate term to allow for non-linear responses of AMF along the seasonal climate gradient. To simplify the analysis and address potential multi-collinearity, we represented climate, biodiversity, and canopy traits using PC1 of their respective variable sets (Section 2.6), so that each factor was summarised by a single composite axis capturing the dominant gradient in that group. We treated gardens as random intercepts in all component models to account for unmeasured site-specific differences in management and environment, while specifying climate, biodiversity, and canopy traits as fixed effects, as their coefficients were the main focus of our inferences.

We fitted each component model as a linear mixed-effects regression using the lme4 R package (Bates et al., 2015), then combined them into a single SEM with the piecewiseSEM package (Lefcheck, 2016). To ensure comparability of coefficients across predictors, all variables, including PC scores and log AMF abundance, were z-standardized (mean 0, standard deviation 1) prior to model fitting (Harrison et al., 2018), the resulting path coefficients therefore represent standardized effects (β). We calculated indirect effects (e.g. climate → biodiversity→ vegetation indices → AMF) as the product of the standardized path coefficients along each route. Their significance was assessed by bootstrap 95% confidence intervals, effects whose intervals did not include zero were considered supported (Table 3-5). Where applicable, global model fit was evaluated using the test of directed separation based on Fisher's C as implemented in the piecewise SEM package (Shipley, 2000), and we further summarised model performance using marginal and conditional $R^2$ for each category. Marginal $R^2$ represents the proportion of variance explained by the fixed effects alone (climate, biodiversity and canopy traits), whereas conditional $R^2$ represents the proportion of variance explained jointly by both fixed and random effects (i.e. including between-garden differences). The comparison between marginal and conditional $R^2$ therefore indicates how much of the explained variation arises from the hypothesised predictors against unmeasured garden-level heterogeneity. Because biodiversity, canopy traits, and AMF were measured almost at the same sampling times, the SEM evaluates hypothesised pathways but it does not prove the direction of causation.

To evaluate the sensitivity of the piecewise SEM to the use of PCA-derived variables, we fitted an alternative non-PCA model. For each predictor group, observed variables were standardized and averaged to create composite climate, biodiversity, vegetation-index, and canopy-height variables. The hypothesised pathways, quadratic climate term, and garden random-intercept structure were otherwise unchanged. We additionally screened log AMF abundance for potential outliers using $|z| > 3$. No observations exceeded this threshold. Results of the sensitivity analysis are presented in Table S4. Statistical assumptions were

**Table 3**
Standardized path coefficients (β) from the piecewise structural equation model relating climate, biodiversity, vegetation indices, canopy height and AMF abundance. Coefficients are based on linear mixed-effects component models with garden included as a random intercept and all continuous variables standardized before model fitting. The AMF component model included both climate PC1 and a quadratic term ($PC1^2$) to capture the non-linear climate–AMF relationship. SE = standard error; df = approximated degrees of freedom; ns = non-significant ($p \geq 0.05$); * $p < 0.05$; ** $p < 0.01$; *** $p < 0.001$.

| Response (endogenous) | Predictor (exogenous) | β | SE | df | p-value | Sig. |
|---|---|---|---|---|---|---|
| Biodiversity | Climate | 0.47 | 0.12 | 129.81 | < 0.001 | *** |
| Vegetation indices | Climate | −0.12 | 0.13 | 126.85 | 0.156 | ns |
| | Biodiversity | −0.41 | 0.08 | 126.86 | < 0.001 | *** |
| Canopy height | Climate | 0.05 | 0.14 | 128.35 | 0.575 | ns |
| | Biodiversity | 0.37 | 0.09 | 128.34 | < 0.001 | *** |
| AMF abundance | Climate (PC1) | −0.51 | 0.15 | 122.50 | < 0.001 | *** |
| | Climate ($PC1^2$) | 0.25 | 0.22 | 124.12 | 0.019 | * |
| | Biodiversity | 0.02 | 0.06 | 122.06 | 0.781 | ns |
| | Vegetation indices | 0.21 | 0.06 | 126.41 | 0.001 | ** |
| | Canopy height | 0.01 | 0.06 | 124.22 | 0.891 | ns |

**Table 4**
Marginal and conditional $R^2$ values for each endogenous variable in the piecewise structural equation model. Marginal $R^2$ quantifies variance explained by fixed effects (climate, biodiversity, vegetation indices and canopy height), whereas conditional $R^2$ reflects variance explained by both fixed effects and the random garden intercept.

| Response variable | $R^2$ marginal | $R^2$ conditional |
|---|---|---|
| Biodiversity | 0.22 | 0.23 |
| Vegetation indices | 0.22 | 0.32 |
| Canopy height | 0.15 | 0.19 |
| AMF abundance | 0.61 | 0.70 |

**Table 5**
Indirect effects from the piecewise structural equation model (SEM) linking climate, biodiversity, UAV-derived vegetation indices and canopy height to arbuscular mycorrhizal fungal (AMF) abundance. These Indirect effects involve CLIM_PC1; the quadratic term ($PC1^2$) enters only the AMF component model and therefore contributes only to the direct climate–AMF relationship. Shown are standardized indirect path coefficients (β) and associated p-values for specific mediating pathways, grouped by predictor. Significance codes: *** $p < 0.001$; ns, not significant.

| Predictor | Mediating pathway | β | p-value | Sig. |
|---|---|---|---|---|
| Climate | Climate → Biodiversity→ AMF | 0.01 | 0.453 | ns |
| Climate | Climate → Vegetation indices → AMF | −0.03 | 0.364 | ns |
| Climate | Climate → Canopy height → AMF | −0.00 | 0.756 | ns |
| Climate | Climate → Biodiversity→ Vegetation indices → AMF | **−0.04** | **< 0.001** | *** |
| Climate | Climate → Biodiversity→ Canopy height → AMF | −0.01 | 0.237 | ns |
| Biodiversity | Biodiversity→ Vegetation indices → AMF | **−0.09** | **< 0.001** | *** |
| Biodiversity | Biodiversity→ Canopy height → AMF | −0.02 | 0.230 | ns |

evaluated separately for each linear mixed-effects component model included in the piecewise SEM. Residual normality was visually assessed using normal Q-Q plots and formally evaluated using Shapiro–Wilk tests. Homoscedasticity was examined using plots of standardized residuals against conditional fitted values and Breusch-Pagan tests. Smoothed residual trends were added to the residual-versus-fitted plots to identify potential systematic patterns. Standardized residuals were additionally screened for extreme values using an absolute threshold of three (Fig. S2).

## 3. Results

### 3.1. Spatiotemporal variation in AMF and environmental effects

AMF abundance differed between years across all gardens (Fig. 3). Distributions in 2021 were consistently shifted upward relative to 2022, indicating higher AMF abundance in the first year at every site. Across all the gardens and sampling dates, log AMF varied substantially over time and among gardens (Fig. 3a). Mean values generally increased from May to midsummer, with the highest values observed in July and August 2021 (≈ 7.1–8.3 log copies $g^{-1}$ dry soil). However, the temporal patterns were not identical across years: July and October 2022 showed consistently lower AMF abundance than the corresponding 2021 sampling periods. In October 2021, FF and KF remained high, whereas ESS and SA declined, indicating that temporal variation was also garden-dependent. These patterns show strong year-to-year and garden-level variation rather than a single uniform seasonal trend.

When we linked AMF abundance to the main pattern in monthly climate conditions, captured by the PC1 from ERA5-Land data (PC1 climate, explaining 81% of the variation), a clear non-linear trend appeared (Fig. 3b). Quadrats with intermediate PC1 values had relatively low AMF abundance, AMF abundance was higher toward both low and high ends of the PC1 gradient (Fig. 3b). By contrast, AMF abundance increased approximately monotonically along the PC1 of plant biodiversity metrics (PC1 biodiversity factors; 70% of variance), which integrates variation in plant species richness and total plant abundance at the quadrat scale (Fig. 3c). Quadrats with higher values of PC1 biodiversity, corresponding to species richer and denser plant communities, tended to exhibit higher log AMF abundance.

### 3.2. Relationships between AMF abundance and UAV-derived canopy metrics

Pairwise correlations between log AMF abundance and individual UAV metrics revealed distinct patterns among metric groups (Fig. 4). Several spectral diversity metrics were significantly related to AMF, with spectral entropy (H_spec) showing negative correlations and some coefficient of variation (CV) and spectral angle mapper (SAM) metrics in the VIS range showing positive correlations. Texture features exhibited a similar mixture of positive and negative correlations depending on band and statistic (contrast, homogeneity, energy, correlation). By contrast, vegetation indices were generally positively associated with AMF and most variables showed significant positive correlations, whereas GCVI was not significant. Both canopy height metrics, height entropy (Hh) and structural richness (Sh), were positively correlated with AMF.

To reduce dimensionality and address collinearity within each metric group, we summarised predictors using PCA and related PC1 scores to log AMF abundance (Fig. 5). For spectral diversity and texture features, PC1 captured 41% and 50% of the variance, respectively, but showed no significant linear association with AMF (spectral diversity: $r = 0.04$, $p = 0.62$; texture: $r = -0.09$, $p = 0.44$). In both cases, PC1 combined metrics with opposing signs of correlation to AMF, which weakened the overall PC1-AMF relationship. Because PC1 summarizes the dominant shared variation among UAV metrics rather than the combination of variables most strongly related to AMF abundance, metrics with positive and negative AMF associations can partly offset one another along the same PC1 axis. In contrast, vegetation indices and canopy-height metrics showed strong within-group correlations and were all positively related to AMF, so their PC1 axes represented coherent gradients of canopy vigour and structure. Accordingly, PC1 for vegetation indices (74% variance explained) and canopy height (85% variance explained) showed significant positive correlations with AMF (vegetation indices: $r = 0.36$, $p < 0.001$; canopy height: $r = 0.29$, $p < 0.001$).

### 3.3. Machine learning prediction of AMF

To evaluate how much variation in AMF abundance can be captured by each UAV metric categoriy when used in multivariate models, we fitted linear regression models with LASSO feature selection and cross-validation separately for spectral diversity metrics, texture features, vegetation indices and canopy-height metrics (Fig. 6). The number of retained predictors was tuned within cross-validation rather than fixed a priori. Across categories, cross-validated $R^2$ values ranged from 0.04 to 0.38. Models based on texture features performed best (test $R^2 = 0.38$, RMSE = 0.79), followed by vegetation indices (test $R^2 = 0.18$, RMSE = 0.97) and spectral diversity metrics (test $R^2 = 0.15$, RMSE = 0.98), whereas canopy-height metrics alone showed very limited predictive power (test $R^2 = 0.04$, RMSE = 1.00). These supervised models indicate that log AMF abundance responds to specific multivariate combinations of UAV metrics rather than to the dominant unsupervised variance axis (PC1), so the absence of a simple PC1-AMF correlation for some categories is compatible with the modest predictive ability observed in the multivariate models, because it uses those specific combinations effectively. The relatively low to moderate cross-validated $R^2$ values indicate that UAV-derived canopy traits captured only part of the spatial variation in AMF abundance. This is ecologically expected because AMF abundance is influenced not only by aboveground canopy greenness, structure, and texture, but also by belowground factors such as plant

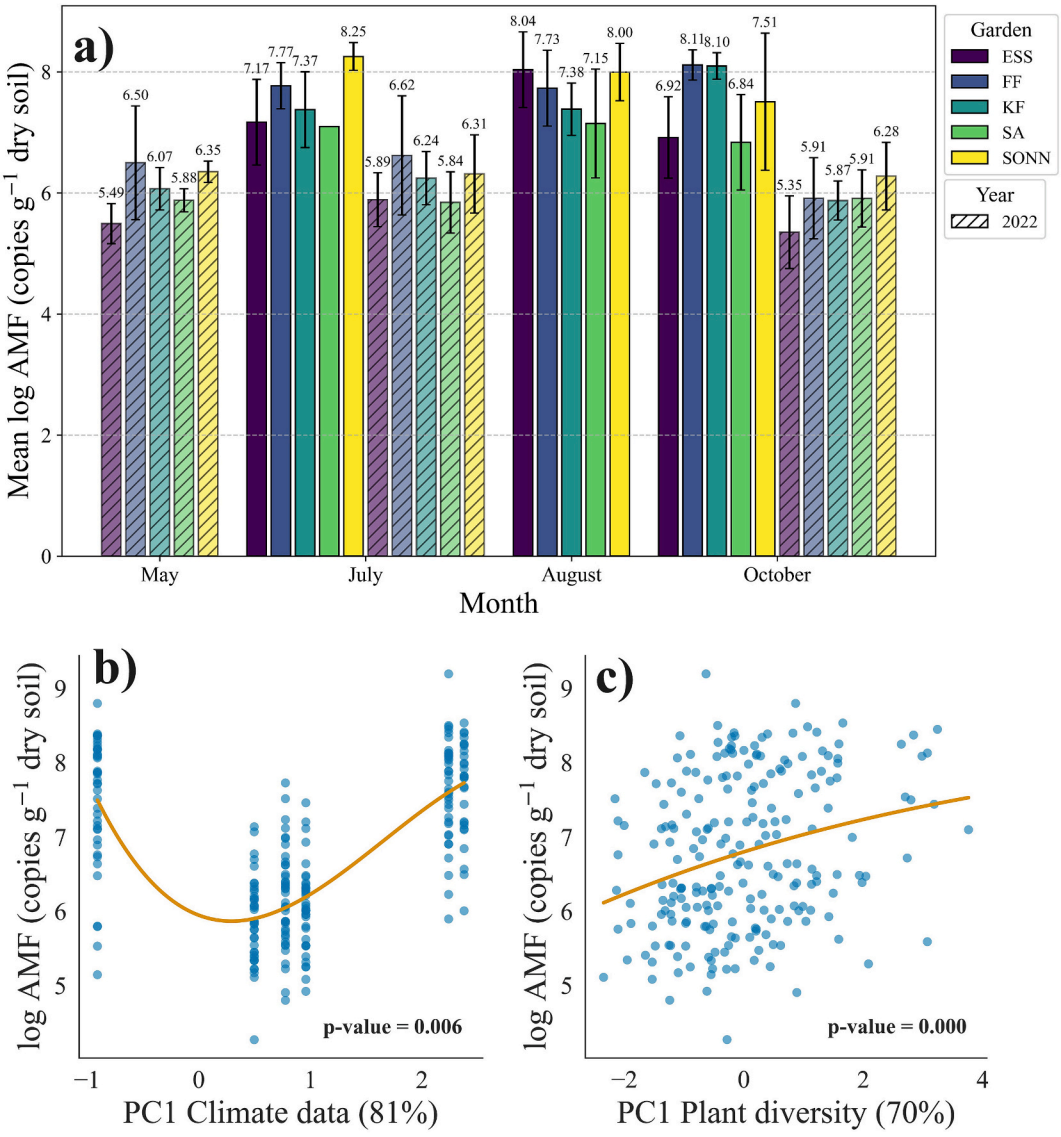


**Fig. 3.** (a) Seasonal and between-garden variation in arbuscular mycorrhizal fungi (AMF) abundance (log copy number $g^{-1}$ dry soil weight) across five urban gardens (Essbare Stadt (ESS), Freihamer Freiluftgarten (FF), Karlsfeld (KF), StadtAcker (SA), and Sonnengarten Solln (SONN)) in 2021 (solid bars) and 2022 (hatched bars). Bars show mean values across quadrats, and error bars indicate ±1 standard error. (b) Relationship between $\log_{10}$ AMF abundance and the first principal component of climate variables, which summarizes monthly air temperature and precipitation. Points represent individual quadrats, with the orange curve showing a smoothed trend. (c) Relationship between $\log_{10}$ AMF abundance and the first principal component of plant biodiversity metrics, integrating plant species richness and total abundance at the quadrat scale. The orange line depicts the fitted trend.

host identity, root distribution, soil properties, microbial interactions, and recent garden management. Therefore, these models should be interpreted as indirect predictive relationships rather than complete explanations of AMF variation. As an additional robustness check, we repeated the modelling workflow using 100 random 80:20 training-testing splits. The ranking of predictor groups remained consistent: texture features showed the highest mean predictive performance ($R^2$ = 0.36 ± 0.17, RMSE = 0.83 ± 0.17), whereas canopy-height metrics showed the weakest performance ($R^2$ = 0.09 ± 0.09, RMSE = 0.99 ± 0.11; Table S2). This confirmed that the main cross-validation results were not dependent on a single data partitioning scheme.

### 3.4. Piecewise structural equation model (SEM)

The piecewise structural equation model clarified how climate, biodiversity and drone-derived canopy traits jointly relate to AMF abundance (Fig. 7; Tables 3–5). The model explained a substantial fraction of variation in AMF (marginal $R^2$ = 0.62, conditional $R^2$ = 0.70), and supported a non-linear association between climate and AMF (CLIM_PC1: β = −0.51, $p < 0.001$; CLIM_PC1$^2$: β = 0.25, $p = 0.019$). In contrast, biodiversity showed no significant direct effect on AMF (β = 0.02, $p = 0.78$) once climate and canopy traits were included, whereas vegetation indices had a moderate positive effect (β = 0.21, $p < 0.001$) and canopy height had no detectable direct effect (β = 0.01, $p = 0.89$). Because the hypothesised network is saturated (all variables are connected by at least one specified path or covariance), no d-separation tests were available and Fisher's C could not be computed; global fit is therefore summarised by the marginal and conditional $R^2$ of the component models rather than a single overall Fisher's C statistic.

Climate also influenced the structure of the plant community and canopy traits. Higher climatic PC1 values were associated with increased biodiversity (β = 0.47, $p < 0.001$; $R^2$_marg = 0.22) but had no significant direct effect on vegetation indices or canopy height. Biodiversity, in turn, was negatively related to the vegetation indices PC1 (β

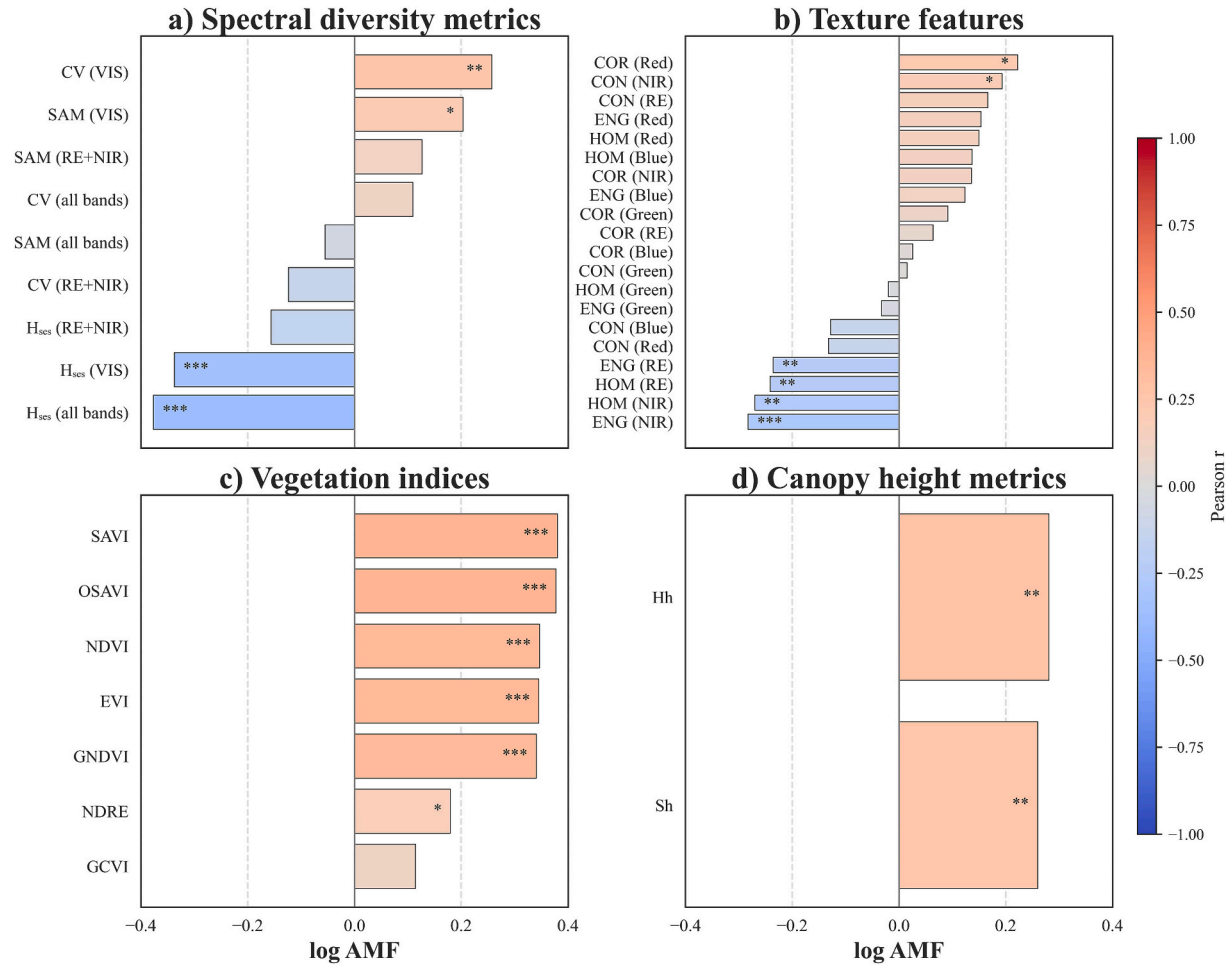


**Fig. 4.** Pearson correlations between log AMF abundance (copy $g^{-1}$ dry soil) and UAV-derived canopy metrics. Panels show (a) spectral diversity metrics, (b) texture features, (c) vegetation indices and (d) canopy height metrics. Spectral diversity metrics include the coefficient of variation (CV; CV all bands, CV VIS, CV RE + NIR), spectral entropy ($H_{spec}$; $H_{spec}$ all bands, $H_{spec}$ VIS, $H_{spec}$ RE + NIR) and spectral angle mapper (SAM; SAM all bands, SAM VIS, SAM RE + NIR). Texture features are grey level co-occurrence matrix (GLCM) statistics: contrast (CON), homogeneity (HOM), energy (ENG) and correlation (COR) calculated for blue, green, red, red-edge (RE) and near-infrared (NIR) bands. Vegetation indices comprise normalized difference vegetation index (NDVI), green NDVI (GNDVI), red-edge NDVI (NDRE), enhanced vegetation index (EVI), soil-adjusted vegetation index (SAVI), optimized SAVI (OSAVI) and green chlorophyll vegetation index (GCVI). Canopy height metrics include height entropy (Hh; foliage height diversity) and structural richness (Sh). Asterisks indicate significance levels: * $p < 0.05$, ** $p < 0.01$, *** $p < 0.001$. (For interpretation of the references to colour in this figure legend, the reader is referred to the web version of this article.)

= −0.41, p < 0.001; $R^2$_marg = 0.22) and positively related to canopy height (β = 0.37, p < 0.001; $R^2$_marg = 0.15). This negative path suggests that species-rich quadrats were not necessarily the greenest, likely reflecting patchy vegetation cover and inconsistent garden management. Indirect-effect calculations showed a small but significant indirect pathway from climate to AMF via biodiversity and vegetation indices (climate→ biodiversity→ vegetation indices → AMF: β = −0.04, p < 0.001), and a similar indirect effect of biodiversity on AMF mediated by vegetation indices (β = −0.09, p < 0.001). Other indirect paths via canopy height were not significant (Table 5). A sensitivity analysis using an alternative path ordering (Climate → vegetation indices → biodiversity) produced qualitatively similar results for AMF, with the same significant Climate → AMF and vegetation indices → AMF paths, indicating that our main conclusions are robust to the assumed ordering of vegetation indices and biodiversity (Table S3).

Replacing PCA-derived predictors with standardized mean composites produced results consistent with the original SEM (Table S4). Climate retained significant linear and quadratic associations with AMF abundance, and vegetation indices remained positively associated with AMF. Biodiversity and canopy-height composites remained non-significant. The alternative model explained a similar proportion of AMF variation to the original model, with marginal $R^2$ = 0.612 and conditional $R^2$ = 0.708. Residual diagnostics generally supported the assumptions of the piecewise SEM component models (Fig. S2). No significant departures from residual normality were detected for the vegetation-index model (Shapiro–Wilk; W = 0.990, $p = 0.428$), canopy-height model (W = 0.991, $p = 0.562$), or AMF model (W = 0.990, $p = 0.493$). Similarly, Breusch-Pagan tests showed no significant evidence of heteroscedasticity for the vegetation-index (chi-squared; $\chi^2 = 1.712$, $p = 0.191$), canopy-height ($\chi^2 = 0.865$, $p = 0.352$), or AMF component models ($\chi^2 = 0.729$, $p = 0.393$). The biodiversity component showed modest departures from residual normality (W = 0.979, $p = 0.039$) and homoscedasticity ($\chi^2 = 6.172$, $p = 0.013$). No standardized residual exceeded an absolute value of three in any component model.

### 3.5. AMF variation among vegetation community types

To evaluate whether host-community identity contributed to AMF variation at the quadrat scale, we performed an additional analysis using field-based plant species-cover data. Community type was significantly associated with log AMF abundance after accounting for garden identity and sampling month (p < 0.001; Fig. 8). Bare/low vegetation cover showed the lowest AMF abundance, whereas grass- and legume-associated quadrats tended to show higher AMF values, indicating that

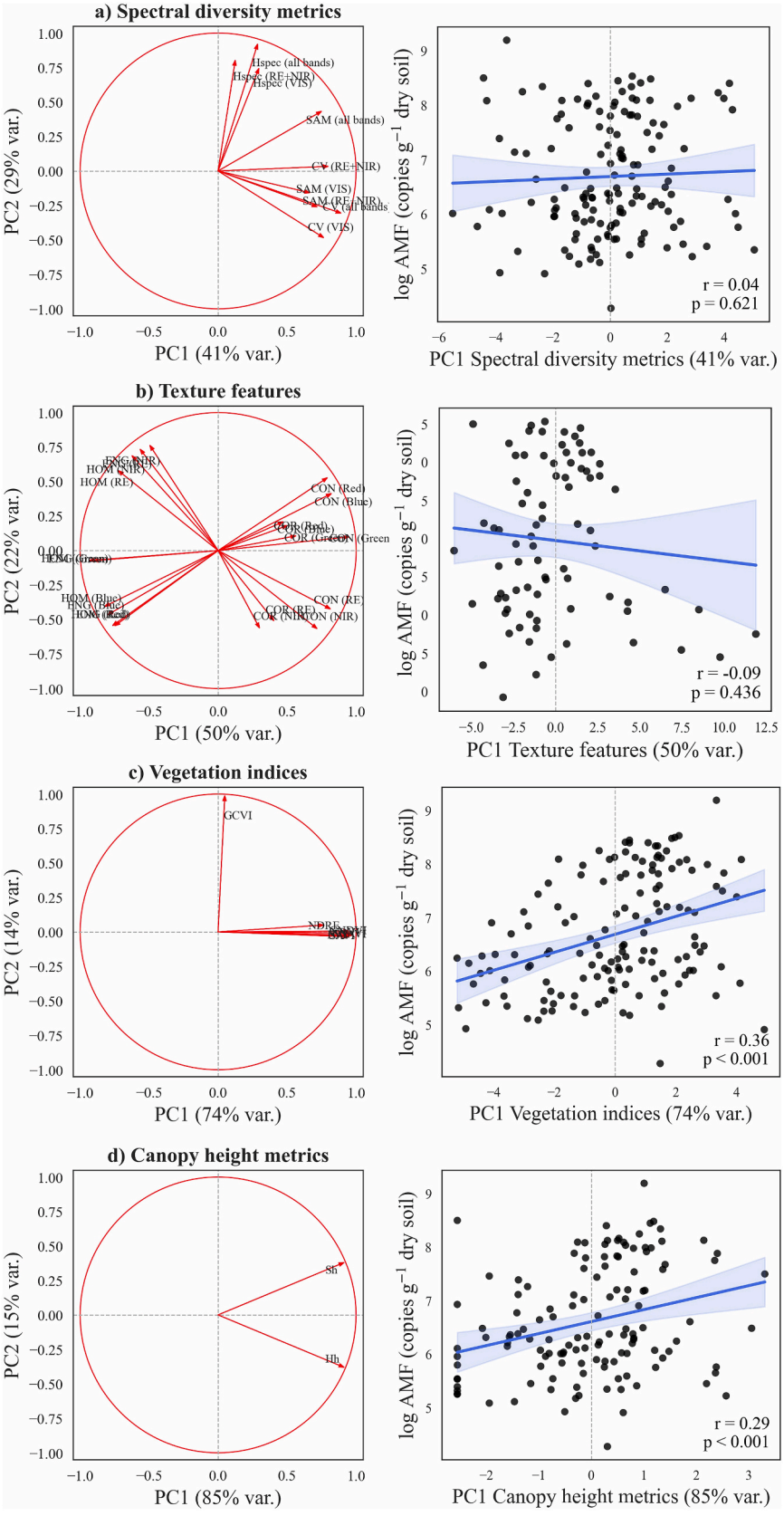


(caption on next page)

**Fig. 5.** Principal component structure and relationships between UAV-derived canopy metrics and arbuscular mycorrhizal fungi (AMF) abundance. Left panels (a-d) show PCA correlation circles for four groups of UAV metrics: (a) spectral diversity metrics, (b) texture features, (c) vegetation indices, and (d) canopy height metrics. Arrows indicate correlation loadings of individual variables on the first two principal components (PC1 and PC2; percentage of variance explained in parentheses). Longer arrows indicate stronger contributions to the PCA axes, while arrows pointing in similar or opposite directions indicate positive or negative correlations among variables, respectively. Right panels show relationships between log AMF abundance (copies $g^{-1}$ dry soil) and PC1 scores for each UAV metric category, with linear regression lines (blue) and 95% confidence bands. Pearson correlation coefficients (r) and associated *p*-values are reported in each scatterplot. (For interpretation of the references to colour in this figure legend, the reader is referred to the web version of this article.)

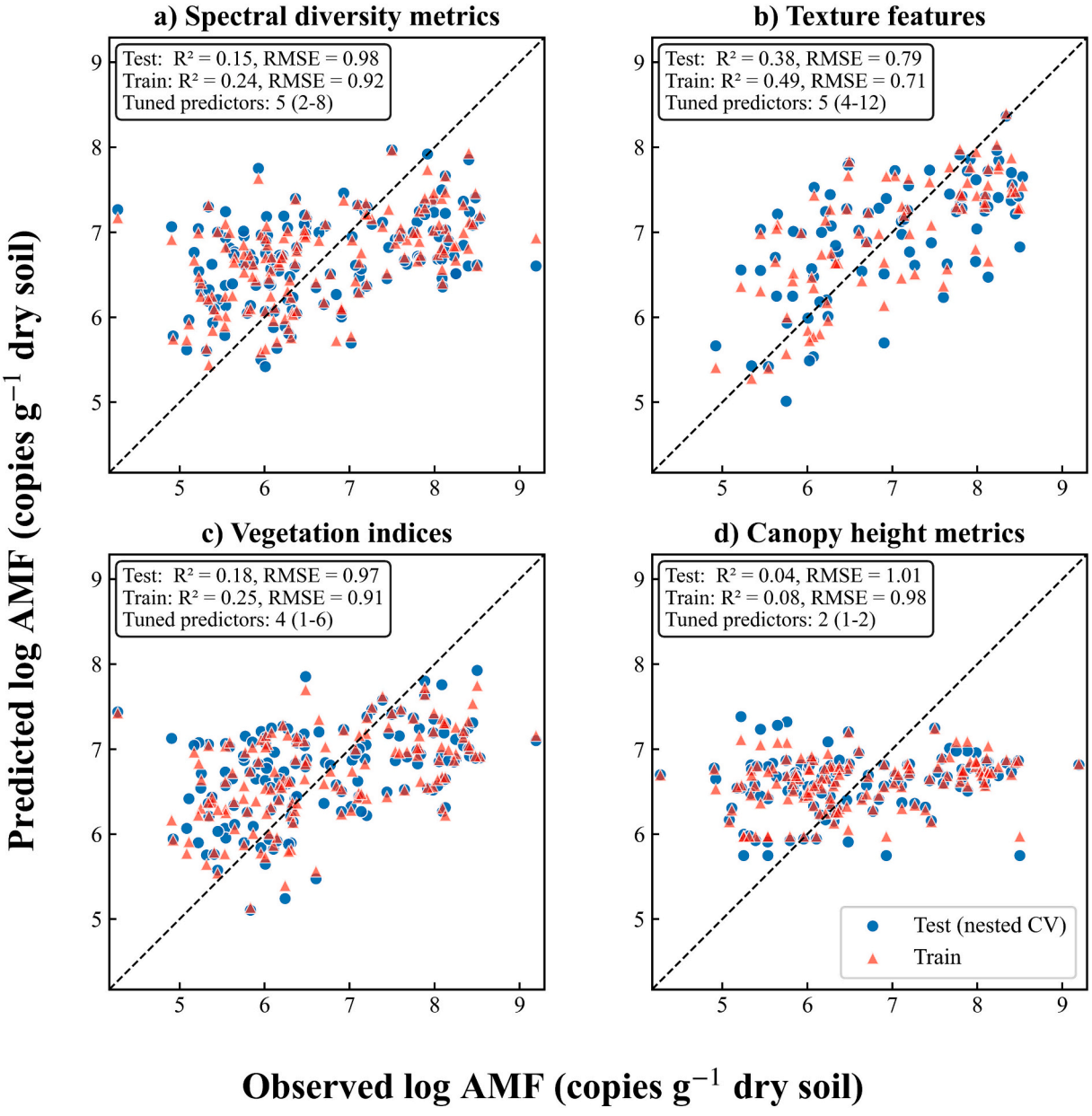


**Fig. 6.** Predicted versus observed arbuscular mycorrhizal fungi (AMF) abundance from category-specific UAV metrics. Panels show cross-validated linear regression models with LASSO feature selection fitted separately to (a) spectral diversity metrics, (b) texture features, (c) vegetation indices and (d) canopy height metrics. Blue circles denote test (out-of-fold) predictions and red triangles denote fits to the full training data; the dashed line indicates 1:1 agreement. Insets report cross-validated ($R^2$, RMSE) and training performance for each model. "Tuned predictors" indicates the median number of retained predictors across cross-validation folds, and values in parentheses indicate the corresponding range across folds. (For interpretation of the references to colour in this figure legend, the reader is referred to the web version of this article.)

host-community context contributed to plot-scale AMF variation.

To further examine species-level host associations, we modelled log AMF abundance as a function of individual species cover for species present in at least eight quadrats, while accounting for garden identity and sampling month (Table S5). Six species showed significant associations after false-discovery-rate correction. AMF abundance was positively associated with the cover of *Mentha* × *piperita*, *Fragaria* × *ananassa*, *Erigeron annuus*, and *Trifolium repens*, and negatively associated with *Pisum sativum* and *Brassica oleracea*. These results provide additional evidence that AMF abundance covaried with plant species

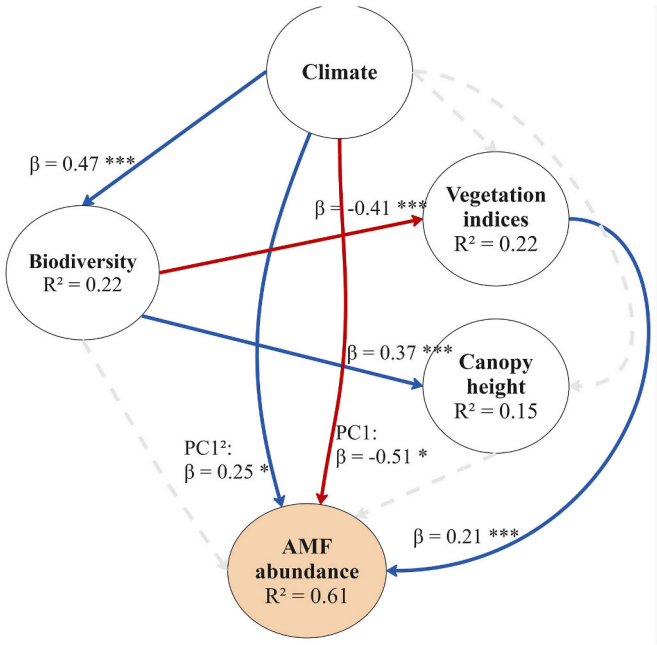


**Fig. 7.** Piecewise structural equation model (SEM) linking climate, biodiversity, UAV-derived canopy traits and arbuscular mycorrhizal fungi (AMF) abundance across urban community gardens. Climate, biodiversity, vegetation indices and canopy height are represented by their first principal component (PC1), summarizing respectively monthly air temperature and precipitation, plant species richness and total abundance, UAV vegetation indices (NDVI, EVI, SAVI, OSAVI, GNDVI, NDRE, GCVI) and UAV-derived canopy height metrics (CHM entropy and height richness). To allow a non-linear climate response, the AMF component model included both climate PC1 and a quadratic term ($PC1^2$). Arrows show standardized path coefficients (β) from mixed-effects linear component models with garden as a random intercept; line width is proportional to $|\beta|$. Solid blue and red arrows indicate significant positive and negative effects ($p < 0.05$), whereas grey dashed arrows indicate non-significant paths or residual covariances ($p \geq 0.05$). $R^2$ values denote marginal $R^2$ (variance explained by fixed effects) for each response variable. (For interpretation of the references to colour in this figure legend, the reader is referred to the web version of this article.)

identity and host-community composition at the 1 $m^2$ scale.

UAV-derived vegetation indices and GLCM texture features also differed among field-defined community types (Fig. S3). Community-type separation was stronger for vegetation indices (PERMANOVA $R^2 = 0.21$, $p = 0.001$) than for GLCM texture features ($R^2 = 0.11$, $p = 0.011$). This indicates that UAV-derived greenness and texture metrics partly captured variation in community structure, although overlap among groups shows that these metrics should be interpreted as indirect indicators rather than exact vegetation-type classifiers.

## 4. Discussion

In this study, our results show that AMF abundance in urban community gardens varies strongly across the growing season and between years, with higher values during warm, high-productivity periods. Across quadrats, AMF abundance was generally higher in quadrats with greener canopies. Texture-based metrics suggested that denser or more patchy canopy structure was also linked to higher AMF, while canopy height metrics contributed little. These patterns show that UAV canopy traits can capture part of the belowground AMF variation. However, these relationships were not strong enough for canopy traits to fully predict AMF. Statistically, this was reflected by low to moderate cross-validated $R^2$ values, indicating limited predictive accuracy when UAV canopy traits were used alone. Ecologically, this limitation is expected because AMF abundance is also shaped by belowground soil conditions, management disturbance and host-root processes that are not fully represented by aboveground canopy structure. The SEM results further suggest that climate conditions are the dominant factor linked to AMF, while biodiversity mostly affects AMF indirectly through canopy traits. In the following sections, we discuss why AMF peaks in warm and productive periods, what UAV traits can and cannot tell us about AMF, and how climate, canopy traits, and biodiversity interact to shape AMF patterns in gardens.

### 4.1. AMF abundance is higher in warm and productive periods

Warming can enhance AMF abundance both directly (by promoting hyphal growth) and indirectly by increasing plant productivity and carbon allocation to fungi (Pérez-Ramos et al., 2021; Xie et al., 2024). The non-linear association between AMF abundance and the climatic PC1 suggests that AMF levels were lowest at intermediate climate PC1 values (i.e., intermediate positions along the seasonal climate gradient) and higher toward both ends of the climate gradient. Because our sampling was restricted to mid-spring to early autumn, and the gardens are regularly irrigated, this climatic gradient reflects variation within the growing season rather than strong drought, and it does not include winter freezing (Xie et al., 2024). This interpretation is consistent with experimental work showing that mild warming combined with a small reduction in precipitation can increase AMF biomass and diversity, whereas stronger warming and greater precipitation reduction can decrease AMF biomass and root colonization (Augé, 2001; Xie et al., 2024). More generally, AMF responses to water stress vary: some studies report little change or even higher colonization under short drought, but other studies show that drought can reduce hyphal density and colonization when water limitation is stronger or longer-lasting (Xiao et al., 2019).

Our observed AMF levels are also within the range reported by soil qPCR studies. For example, a karst grassland study reported $7.20 \times 10^7$ to $1.92 \times 10^8$ copies $g^{-1}$ dry soil ($\log_{10}$ 7.86–8.28), while a cropland dataset reported AMF gene copy numbers around $1.2 \times 10^6$ to $2.1 \times 10^8$ copies $g^{-1}$ soil ($\log_{10}$ 6.08–8.32) (Xiao et al., 2019). In our gardens, the seasonal increase in AMF toward summer therefore fits a simple explanation: when plants grow faster in warm months, they tend to send more carbon to roots and associated AMF, while local differences among quadrats likely reflect additional factors such as soil conditions and uneven management (Lange et al., 2015b).

Our results indicate that AMF abundance was positively associated with observed plant species richness and overall plant abundance (PC1 biodiversity) at the quadrat level. This pattern is consistent with the idea that more species diverse and denser plant assemblages supply larger and more continuous inputs of photosynthate and root exudates to the rhizosphere, supporting more extensive soil microbial networks and thereby facilitating AMF proliferation (Chen et al., 2019; Lange et al., 2015b). However, these simple relationships overlook overlaps with local climate and canopy structure (Fig. 7). In these sampled gardens, quadrats with more species-diverse plant assemblages often occurred in warmer sampling periods, more productive spots with higher vegetation indices and canopy heights, suggesting shared effects of seasonal climate and local microclimate and management. Thus, part of the biodiversity-AMF association may reflect a shared resource and microclimate gradient rather than diversity alone. In our study, this highlights that boosting biodiversity in community gardens can support AMF, but its success depends on interactions with local microclimate and management, which together determine the actual AMF response.

### 4.2. UAV-derived canopy health and fine-scale heterogeneity only partly predict AMF abundance

AMF abundance tended to be higher in quadrats with greener, denser foliage and more structurally complex canopies. Drone-derived vegetation indices such as SAVI, OSAVI, NDVI, EVI and related chlorophyll-

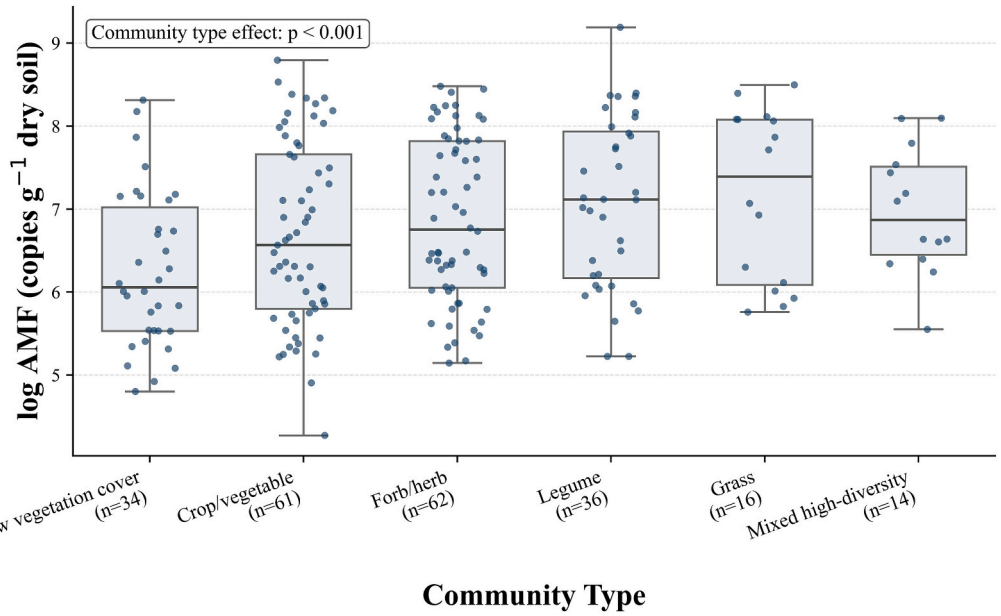


**Fig. 8.** Variation in arbuscular mycorrhizal fungal abundance among field-defined host-community types. Each point represents one quadrat, and boxplots show the median, interquartile range, and distribution of log AMF abundance. Community types were classified using field survey data. Numbers below the x-axis (n) indicate the number of quadrats included in each host-community type.

sensitive metrics provide compact proxies for canopy health, leaf area and photosynthetic activity, which are tightly linked to carbon inputs belowground (Sørensen et al., 2025). Soil-adjusted indices like SAVI and OSAVI are less affected by soil background than other vegetation indices in patchy canopies, and therefore may better track the effective green biomass that fuels AMF through carbon allocation to roots and rhizosphere exudation (Huete, 1988). Consistent with this mechanism, all chlorophyll-sensitive indices showed positive correlations with AMF abundance, and the vegetation-index model explained about 20% of cross-validated variance in AMF.

Our results show that CHMs metrics captured additional aspects of stand structure. Height entropy and structural richness reflect variation in the distribution of vegetation height within quadrats and are often associated with greater plant species richness, more complex rooting architectures and enhanced microclimate buffering in structurally diverse stands (Lang et al., 2023). Although canopy height metrics and their principal component showed positive univariate associations with AMF abundance, their predictive power using ML model was limited (explaining only about 5% of the AMF abundance changes). In this specific urban garden system, canopy height likely performed poorly because vegetation was generally low-stature, frequently managed and spatially patchy within quadrats. Under these conditions, small differences in canopy height do not necessarily reflect differences in host-root biomass, AMF host quality or belowground fungal habitat. This limitation can be attributed to a weak overall correlation between height metrics and AMF. In urban gardens, where plant height is generally modest with minimal height variation, these metrics serve only as rough proxies for more complex factors such as root mass and plant community composition, but require further corroboration. For example Lang et al. (2023) showed that canopy structural metrics can correlate with the richness and composition of soil fungal and mycorrhizal communities. But they also state explicitly that soil properties were the strongest predictors of microbial richness and composition compared with structural diversity and tree species diversity. Canopy height therefore represents only one layer of the multiple interacting controls on AMF abundance.

Beyond canopy health, greenness, and canopy height metrics, our UAV spectral-diversity and texture features captured fine-scale heterogeneity in reflectance and horizontal structure. The spectral variability hypothesis proposes that higher variation in spectral signatures could mirror higher habitat and plant species diversity, because different species and functional types occupy distinct spectral characteristics (Palmer et al., 2002; Rocchini et al., 2004; Schweiger et al., 2018). In line with our assumption, our results showed that GLCM-based texture features explained up to ~38% of cross-validated variance in AMF abundance, which is moderate for belowground biodiversity, and outperformed other UAV-derived canopy traits (vegetation indices, canopy height, and spectral diversity). Texture features (contrast, homogeneity, energy and correlation) may be linked to spatial arrangement of host plants and patterns like gaps, edges and clumped foliage that co-vary with root density, litter inputs and shaded, moist microsites where AMF grow by extending hyphae and producing spores. In addition, texture in the NIR and red-edge bands is particularly sensitive to leaf area index, leaf structure and canopy moisture, and therefore to gradients in biomass and rooting density that govern the amount and continuity of carbon flow to AMF networks (Lang et al., 2023). By contrast, spectral-diversity metrics showed weaker performance compared to texture features and vegetation indices. In these intensively managed gardens, spectral diversity likely captured mixed sources of reflectance variation, including bare soil, paths, crop residues, weeds and non-host vegetation, in addition to functional differences among host plants. This reduces the specificity of spectral diversity as an indicator of AMF habitat compared with texture features, which better captured the spatial arrangement of canopy patches. Climate conditions dominate effects on AMF.

Although AMF abundance was positively correlated with biodiversity at the plot scale, this association did not persist as a direct effect in the SEM once climate and UAV-derived canopy traits were included, indicating that the positive correlation between biodiversity and AMF largely reflects shared responses to seasonal climate variation and associated canopy development. In the SEM, the climate→AMF relationship was non-linear (CLIM_PC1 and CLIM_PC1$^2$), indicating that AMF abundance was lowest at intermediate positions along the climate gradient after accounting for canopy greenness and biodiversity. Because AMF, biodiversity, and canopy traits were measured at the same time, the SEM shows patterns consistent with our proposed pathways but cannot prove which one causes the other. Biodiversity influenced AMF primarily indirectly via canopy traits (canopy greenness and

structure), which in turn were linked to AMF abundance. This suggests that diversity effects on AMF in these gardens are expressed mainly via changes in vegetation functional traits rather than through a simple one-to-one relationship between plant species richness and AMF. The stability of the principal SEM pathways after replacing PCA scores with standardized mean composites indicates that the conclusions were not dependent on the selected variable-aggregation method. Nevertheless, these results represent associations within the sampled gardens and should not be interpreted as evidence of causation.

These SEM-based patterns are consistent with recent findings that show AMF abundance and diversity arise from the interplay of climate, soil properties, land use and host-plant attributes rather than from any single driver (Ma et al., 2023; Van Nuland et al., 2025). In regional and local studies, soil moisture, pH, organic matter, and nitrogen have been shown to significantly influence AMF communities, often overshadowing the impacts of biodiversity (Ma et al., 2021; Zhou et al., 2022). Vályi et al. (2015) found that land-use intensity can interact with host plant identity to influence AMF community structures, where more intensive practices often lead to a decline in AMF diversity. Nutrient enrichment, especially higher P availability from fertilization, is often associated with reduced AMF colonization and lower AMF abundance and diversity. Over-fertilization can intensify this imbalance by reducing plant dependence on AMF for nutrient uptake, leading to suppressed fungal colonization, altered soil microbial dynamics, and ultimately compromised soil health (Lekberg et al., 2021). Because we did not quantify fertiliser inputs or soil nutrients, we could not test this mechanism in our gardens. Given that AMF abundance is jointly driven by host plant community, soil chemistry, moisture, management, and microclimate, we do not expect canopy traits alone to yield high predictive power. Our results instead show that UAV-derived metrics provide additional, remote-sensing accessible information about AMF beyond random variation, but cannot replace direct measurements or detailed environmental data.

### 4.3. Vegetation identity improves ecological interpretation of AMF variation

The additional host-community analysis supports the interpretation that plant identity is an important fine-scale ecological context for AMF abundance in urban gardens. Bare/low vegetation quadrats had the lowest AMF abundance, consistent with reduced living root cover and lower host availability. In contrast, grass- and legume-associated quadrats tended to show higher AMF abundance, suggesting that host functional identity and living plant cover contributed to AMF variation at the 1 $m^2$ scale. Species-level models further showed that AMF abundance was associated with the cover of several individual plant species after accounting for garden identity and sampling month. Positive associations with species such as *Trifolium repens*, *Mentha* × *piperita*, *Fragaria* × *ananassa*, and *Erigeron annuus*, and negative associations with *Pisum sativum* and *Brassica oleracea*, indicate that AMF abundance varied with local host-community composition. These species-level results should be interpreted as observational associations rather than causal species effects. Importantly, UAV vegetation indices and GLCM texture features differed among field-defined community types, indicating that canopy greenness and texture partly captured vegetation-community structure. This strengthens the ecological interpretation of the UAV-based analyses: UAV metrics should not be interpreted as direct measurements of AMF or exact plant species identity, but as indirect indicators of vegetation cover, canopy condition, and spatial structure that are partly linked to AMF-relevant host-community differences. Exact within-quadrat species classification is beyond the scope and capability of the UAV imagery used here and was not an objective of this study.

### 4.4. Ecological indicator, limitations and future directions

Our results suggest that urban community gardens can support high AMF abundance when warm, productive growing conditions coincide with dense, species diverse/rich vegetation and structurally heterogeneous canopies. Management practices that maintain continuous green cover (e.g. by reducing bare soil and using staggered planting), avoid excessive fertilization and irrigation regimes that prevent severe drought while still allowing moderate stress are likely to favour AMF and associated soil functions. However, because diversity effects on AMF are largely mediated through canopy traits and climate, simply increasing plant species richness without considering microclimate, soil conditions and management intensity may yield weaker benefits than expected.

Unmeasured drivers likely explain remaining AMF variation. Even after accounting for canopy traits and seasonal climate, a large share of AMF variation remained unexplained, suggesting additional controls. These factors likely include the soil's chemical and physical characteristics (e.g., nutrients, pH, organic matter, texture), historical land use, and specific garden management techniques (e.g. irrigation and fertilization), which are known to affect AMF in agricultural and urban soils (Kozjek et al., 2021; Liu et al., 2022; Qin et al., 2015). While we did not quantify nutrient inputs or measure management factors in this study, future research can investigate soil management-AMF relationships.

Drone-derived canopy traits (vegetation indices, texture metrics and canopy-height measures) captured ecologically meaningful but only moderate fractions of variation in AMF abundance. This indicates that UAV-based canopy traits can provide a scalable, non-destructive ecological indicator for mapping relative differences in AMF across small urban landscapes and for targeting more intensive belowground sampling. However, our results showed that canopy traits should be considered as complementary indicators that add information, rather than as stand-alone replacements for direct environmental and soil measurements.

The study is restricted to five irrigated community gardens in a single temperate city, dominated by herbaceous vegetation (mostly <1–2 m tall), and covers only two growing seasons, so the results may not generalise to taller, water-limited or less managed systems. On the other hand, AMF were quantified as gene copy numbers, without information on community composition, colonization intensity or functional traits, and important covariates such as soil chemistry, historical management were not explicitly considered. These constraints likely contribute to the unexplained variance in AMF abundance and caution against extrapolating quantitative effect sizes beyond comparable urban gardening contexts.

Building on this work, future studies could (i) integrate UAV data with detailed measurements of soil properties, microclimate and management to assess their relative contributions to AMF dynamics; (ii) expand the remote sensing approach to hyperspectral and LiDAR sensors to capture finer biochemical and structural traits; (iii) couple qPCR-based abundance estimates with metabarcoding biomarkers (which reveals community composition and diversity) to link canopy traits to AMF community composition and function; and (iv) test causality using controlled experiments that vary biodiversity, fertilization and irrigation while repeatedly mapping canopy traits and AMF responses through time. This approach would help pinpoint exactly when and where drone data can accurately reveal underground fungal health in diverse urban areas.

## 5. Conclusions

This study shows that AMF abundance in urban community gardens was highest during warm, productive periods and in quadrats with dense and species rich/diverse vegetation, but that these relationships are largely mediated by climate and canopy traits rather than by biodiversity (species richness) alone. Drone-derived vegetation indices and texture metrics captured ecologically meaningful, yet only moderate, fractions of variation in AMF abundance. The structural equation model further highlighted climate as the dominant driver of AMF, with

biodiversity primarily having indirect effects through its impact on canopy greenness and structure.

Collectively, these results suggest that UAV-based canopy traits offer a useful, scalable ecological indicator for assessing spatial variation in AMF abundance in urban community gardens, although they cannot replace direct soil and environmental assessments in the field. Future research combining UAV data with detailed soil, microclimate and community information, while extending to AMF community composition and controlled experiments, will be useful to refine when and where aboveground canopy signals can reliably inform belowground mycorrhizal status.

## CRediT authorship contribution statement

**Yasamin Afrasiabian:** Writing – review & editing, Writing – original draft, Visualization, Validation, Methodology, Investigation, Formal analysis, Data curation, Conceptualization. **Diana Rocío Andrade-Linares:** Writing – review & editing, Methodology, Data curation. **Stefanie Schulz:** Writing – review & editing, Methodology, Data curation. **Michael Schloter:** Writing – review & editing, Methodology, Data curation. **Elisa Van Cleemput:** Writing – review & editing, Supervision, Methodology, Conceptualization. **Monika Egerer:** Writing – review & editing, Validation, Supervision, Methodology, Funding acquisition, Conceptualization. **Kang Yu:** Writing – review & editing, Validation, Supervision, Resources, Methodology, Funding acquisition, Conceptualization.

## Declaration of generative AI and AI-assisted technologies in the writing process

During the preparation of this work, the authors used ChatGPT to improve the language. After using this tool, the authors reviewed and edited the content as needed and take full responsibility for the content of the publication.

## Declaration of competing interest

The authors declare that they have no known competing financial interests or personal relationships that could have appeared to influence the work reported in this paper.

## Acknowledgements

This work was supported by the Hans Eisenmann-Forum für Agrarwissenschaften (HEF) Seed Fund 2021. The authors thank Ali Mokhtari, Jürgen Pluss, Jie Wang, Haibo Yang, Weilong Qin, Nina Schäle, Michael Miesl, Julia Schmack, Yannick Hecher, Veronica Sebald, Astrid Neumann, Hien Nguyen, and Felix Conitz for their assistance in data collection. We gratefully acknowledge Noureldin Sharaf and Jonathan Christian Maria Ruf for their contributions to the laboratory procedures, including DNA extraction and qPCR.

## Appendix A. Supplementary data

Supplementary data to this article can be found online at https://doi.org/10.1016/j.ecolind.2026.115283.

## Data availability

Data will be made available on request.

## References

Afrasiabian, Y., Contiz, F., Van Cleemput, E., Egerer, M., Yu, K., 2025. Biodiversity monitoring in urban community gardens using proximal sensing and drone remote sensing. Remote Sens. Appl.: Soc. Environ. 39, 101685. https://doi.org/10.1016/J.RSASE.2025.101685.

Andrade-Linares, D.R., Schwerdtner, U., Schulz, S., Dannenmann, M., Spohn, M., Baum, C., Gasche, R., Wiesmeier, M., Garcia-Franco, N., Schloter, M., 2023. Climate change and management intensity alter spatial distribution and abundance of P mineralizing bacteria and arbuscular mycorrhizal fungi in mountainous grassland soils. Soil Biol. Biochem. 186, 109175. https://doi.org/10.1016/j.soilbio.2023.109175.

Augé, R.M., 2001. Water relations, drought and vesicular-arbuscular mycorrhizal symbiosis. Mycorrhiza 11, 3–42. https://doi.org/10.1007/S005720100097/METRICS.

Bates, D., Mächler, M., Bolker, B.M., Walker, S.C., 2015. Fitting linear mixed-effects models using lme4. J. Stat. Softw. 67, 1–48. https://doi.org/10.18637/JSS.V067.I01.

Bell, C.A., Magkourilou, E., Ault, J.R., Urwin, P.E., Field, K.J., 2024. Phytophagy impacts the quality and quantity of plant carbon resources acquired by mutualistic arbuscular mycorrhizal fungi. Nat. Commun. 15, 1–14. https://doi.org/10.1038/S41467-024-45026-3;TECHMETA.

Brundrett, M.C., Tedersoo, L., 2018. Evolutionary history of mycorrhizal symbioses and global host plant diversity. New Phytol. 220, 1108–1115. https://doi.org/10.1111/NPH.14976.

Cavender-Bares, J., Schweiger, A.K., Gamon, J.A., Gholizadeh, H., Helzer, K., Lapadat, C., Madritch, M.D., Townsend, P.A., Wang, Z., Hobbie, S.E., 2021. Remotely detected aboveground plant function predicts belowground processes in two prairie diversity experiments. Ecol. Monogr. 92, e01488. https://doi.org/10.1002/ECM.1488.

Cavender-Bares, J., Schweiger, A.K., Gamon, J.A., Gholizadeh, H., Helzer, K., Lapadat, C., Madritch, M.D., Townsend, P.A., Wang, Z., Hobbie, S.E., 2022. Remotely detected aboveground plant function predicts belowground processes in two prairie diversity experiments. Ecol. Monogr. 92, e01488. https://doi.org/10.1002/ecm.1488.

Chen, C., Chen, H.Y.H., Chen, X., Huang, Z., 2019. Meta-analysis shows positive effects of plant diversity on microbial biomass and respiration. Nat. Commun. 101 (10), 1332. https://doi.org/10.1038/s41467-019-09258-y.

Copernicus Climate Change Service, 2019. ERA5-Land Hourly Data from 1950 to Present. Copernicus Clim. Chang. Serv. Clim. Data Store.

De Deyn, G.B., Van Der Putten, W.H., 2005. Linking aboveground and belowground diversity. Trends Ecol. Evol. 20, 625–633. https://doi.org/10.1016/j.tree.2005.08.009.

Egidi, E., Bristol, D., Hassan, K., Tissue, D., Wright, I.J., Nielsen, U.N., 2025. The influence of plant traits on soil microbial communities varies between arid and mesic grasslands. Plant Soil 509, 501–521. https://doi.org/10.1007/S11104-024-06876-4/FIGURES/6.

Fisher, J.B., Sweeney, S., Brzostek, E.R., Evans, T.P., Johnson, D.J., Myers, J.A., Bourg, N. A., Wolf, A.T., Howe, R.W., Phillips, R.P., 2016. Tree-mycorrhizal associations detected remotely from canopy spectral properties. Glob. Chang. Biol. 22, 2596–2607. https://doi.org/10.1111/GCB.13264.

Forero, L.E., Kulmatiski, A., Grenzer, J., Norton, J.M., 2021. Plant-soil feedbacks help explain biodiversity-productivity relationships. Commun. Biol. 4, 789. https://doi.org/10.1038/S42003-021-02329-1;SUBJMETA.

Gitelson, A.A., Kaufman, Y.J., Merzlyak, M.N., 1996. Use of a green channel in remote sensing of global vegetation from EOS-MODIS. Remote Sens. Environ. 58, 289–298. https://doi.org/10.1016/S0034-4257(96)00072-7.

Gitelson, A., Merzlyak, M.N., 1994. Spectral reflectance changes associated with autumn senescence of *Aesculus hippocastanum* L. and *Acer platanoides* L. leaves. Spectral features and relation to chlorophyll estimation. Journal of Plant Physiology 143, 286–292. https://doi.org/10.1016/S0176-1617(11)81633-0.

Gitelson, A.A., Vina, A., Arkebauer, T.J., Rundquist, D.C., Keydan, G., Leavitt, B., 2003. Remote estimation of leaf area index and green leaf biomass in maize canopies. In: Wiley online Libr. Gitelson, a Viña, TJ Arkebauer, DC Rundquist, G Keydan, B LeavittGeophysical res. Lett. 2003•Wiley online Libr, 30, p. 1248. https://doi.org/10.1029/2002GL016450.

Gollotte, A., Van Tuinen, D., Atkinson, D., 2004. In: Gollotte, SpringerA, Van Tuinen, D., AtkinsonMycorrhiza, D. (Eds.), Diversity of arbuscular mycorrhizal fungi colonising roots of the grass species *Agrostis capillaris* and *Lolium perenne* in a field experiment, 14. Springer, pp. 111–117. https://doi.org/10.1007/s00572-003-0244-7.

Guo, J., Wei, B., Liu, J., Eissenstat, D.M., Yu, S., Gong, X., Wu, J., He, X., Yu, M., 2023. Linkages between plant community composition and soil microbial diversity in Masson pine forests. Plants 12, 1750. https://doi.org/10.3390/PLANTS12091750/S1.

Haralick, R.M., Dinstein, I., Shanmugam, K., 1973. Textural features for image classification. IEEE Trans. Syst. Man Cybern. SMC-3, 610–621. https://doi.org/10.1109/TSMC.1973.4309314.

Harris, A., Bardgett, R.D., 2025. Canopy reflectance as a predictor of soil microbial community composition and diversity at a continental scale. New Phytol. 249, 829. https://doi.org/10.1111/nph.70720.

Harrison, X.A., Donaldson, L., Correa-Cano, M.E., Evans, J., Fisher, D.N., Goodwin, C.E. D., Robinson, B.S., Hodgson, D.J., Inger, R., 2018. A brief introduction to mixed effects modelling and multi-model inference in ecology. PeerJ, e4794. https://doi.org/10.7717/PEERJ.4794/FIG-3.

Helber, N., Wippel, K., Sauer, N., Schaarschmidt, S., Hause, B., Requena, N., 2011. A versatile monosaccharide transporter that operates in the arbuscular mycorrhizal fungus Glomus sp is crucial for the symbiotic relationship with plants. Plant Cell 23, 3812–3823. https://doi.org/10.1105/TPC.111.089813.

Huete, A.R., 1988. A soil-adjusted vegetation index (SAVI). Remote Sens. Environ. 25, 295–309. https://doi.org/10.1016/0034-4257(88)90106-X.

Huete, A., Didan, K., Miura, T., Rodriguez, E.P., Gao, X., Ferreira, L.G., 2002. Overview of the radiometric and biophysical performance of the MODIS vegetation indices.

Remote Sensing of Environment 83, 195–213. https://doi.org/10.1016/S0034-4257(02)00096-2.
Igiehon, N.O., Babalola, O.O., 2018. Below-ground-above-ground plant-microbial interactions: focusing on soybean, rhizobacteria and mycorrhizal Fungi. Open Microbiol. J. 12, 261–279. https://doi.org/10.2174/1874285801812010261.
Jiang, Y., Luan, L., Hu, K., Liu, M., Chen, Z., Geisen, S., Chen, X., Li, H., Xu, Q., Bonkowski, M., Sun, B., 2020. Trophic interactions as determinants of the arbuscular mycorrhizal fungal community with cascading plant-promoting consequences. Microbiome 8, 1–14. https://doi.org/10.1186/S40168-020-00918-6/FIGURES/6.
Kardol, P., Wardle, D.A., 2010. How understanding aboveground–belowground linkages can assist restoration ecology. Trends Ecol. Evol. 25, 670–679. https://doi.org/10.1016/J.TREE.2010.09.001.
Kozjek, K., Kundel, D., Kushwaha, S.K., Olsson, P.A., Ahrén, D., Fliessbach, A., Birkhofer, K., Hedlund, K., 2021. Long-term agricultural management impacts arbuscular mycorrhizal fungi more than short-term experimental drought. Appl. Soil Ecol. 168, 104140. https://doi.org/10.1016/J.APSOIL.2021.104140.
Kruse, F.A., Lefkoff, A.B., Boardman, J.W., Heidebrecht, K.B., Shapiro, A.T., Barloon, P. J., Goetz, A.F.H., 1993. The spectral image processing system (SIPS)—interactive visualization and analysis of imaging spectrometer data. Remote Sens. Environ. 44, 145–163. https://doi.org/10.1016/0034-4257(93)90013-N.
Lang, A.K., LaRue, E.A., Kivlin, S.N., Edwards, J.D., Phillips, R.P., Gallion, J., Kong, N., Parker, J.D., McCormick, M.K., Domke, G., Fei, S., 2023. Forest structural diversity is linked to soil microbial diversity. Ecosphere 14, e4702. https://doi.org/10.1002/ECS2.4702;ISSUE:ISSUE:DOI.
Lange, M., Eisenhauer, N., Sierra, C.A., Bessler, H., Engels, C., Griffiths, R.I., Mellado-Vázquez, P.G., Malik, A.A., Roy, J., Scheu, S., Steinbeiss, S., Thomson, B.C., Trumbore, S.E., Gleixner, G., 2015a. Plant diversity increases soil microbial activity and soil carbon storage. Nat. Commun. 6, 1–8. https://doi.org/10.1038/NCOMMS7707;TECHMETA.
Lange, M., Eisenhauer, N., Sierra, C.A., Bessler, H., Engels, C., Griffiths, R.I., Mellado-Vázquez, P.G., Malik, A.A., Roy, J., Scheu, S., Steinbeiss, S., Thomson, B.C., Trumbore, S.E., Gleixner, G., 2015b. Plant diversity increases soil microbial activity and soil carbon storage. Nat. Commun. 61 (6), 6707. https://doi.org/10.1038/ncomms7707.
Lefcheck, J.S., 2016. PiecewiseSEM: piecewise structural equation modelling in r for ecology, evolution, and systematics. Methods Ecol. Evol. 7, 573–579. Doi: 10.1111/2041-210X.12512;REQUESTEDJOURNAL:JOURNAL:2041210X;WEBSITE:WEBSITE:BESJOURNALS;WGROUP:STRING:PUBLICATION.
Lekberg, Y., Arnillas, C.A., Borer, E.T., Bullington, L.S., Fierer, N., Kennedy, P.G., Leff, J. W., Luis, A.D., Seabloom, E.W., Henning, J.A., 2021. Nitrogen and phosphorus fertilization consistently favor pathogenic over mutualistic fungi in grassland soils. Nat. Commun. 121 (12), 3484. https://doi.org/10.1038/s41467-021-23605-y.
Li, W., Li, D., Warner, T.A., Liu, S., Baret, F., Yang, P., Jiang, J., Dong, M., Cheng, T., Zhu, Y., Cao, W., Yao, X., 2025. Improved generality of wheat green LAI models through mitigation of the effect of leaf chlorophyll content variation with red edge vegetation indices. Remote Sens. Environ. 318, 114589. https://doi.org/10.1016/J.RSE.2024.114589.
Liu, W., Ma, K., Wang, X., Wang, Z., Negrete-Yankelevich, S., 2022. Effects of no-tillage and biologically-based organic fertilizer on soil arbuscular mycorrhizal fungal communities in winter wheat field. Appl. Soil Ecol. 178, 104564. https://doi.org/10.1016/J.APSOIL.2022.104564.
Ludwig, A., Doktor, D., Feilhauer, H., 2024. Is spectral pixel-to-pixel variation a reliable indicator of grassland biodiversity? A systematic assessment of the spectral variation hypothesis using spatial simulation experiments. Remote Sens. Environ. 302. https://doi.org/10.1016/j.rse.2023.113988.
Ma, X., Geng, Q., Zhang, H., Bian, C., Chen, H.Y.H., Jiang, D., Xu, X., 2021. Global negative effects of nutrient enrichment on arbuscular mycorrhizal fungi, plant diversity and ecosystem multifunctionality. New Phytol. 229, 2957–2969. https://doi.org/10.1111/NPH.17077;ISSUE:ISSUE:DOI.
Ma, X., Xu, X., Geng, Q., Luo, Y., Ju, C., Li, Q., Zhou, Y., 2023. Global arbuscular mycorrhizal fungal diversity and abundance decreases with soil available phosphorus. Glob. Ecol. Biogeogr. 32, 1423–1434. https://doi.org/10.1111/GEB.13704;ISSUE:ISSUE:DOI.
McElhinny, C., Gibbons, P., Brack, C., Bauhus, J., 2005. Forest and woodland stand structural complexity: its definition and measurement. For. Ecol. Manag. 218, 1–24. https://doi.org/10.1016/j.foreco.2005.08.034.
Mummey, D.L., Rillig, M.C., 2007. Evaluation of LSU rRNA-gene PCR primers for analysis of arbuscular mycorrhizal fungal communities via terminal restriction fragment length polymorphism analysis. Journal of Microbiological Methods 70, 200–204. https://doi.org/10.1016/j.mimet.2007.04.002.
Muñoz-Sabater, J., Dutra, E., Agustí-Panareda, A., Albergel, C., Arduini, G., Balsamo, G., Boussetta, S., Choulga, M., Harrigan, S., Hersbach, H., Martens, B., Miralles, D.G., Piles, M., Rodríguez-Fernández, N.J., Zsoter, E., Buontempo, C., Thépaut, J.N., 2021. ERA5-land: a state-of-the-art global reanalysis dataset for land applications. Earth Syst. Sci. Data 13, 4349–4383. https://doi.org/10.5194/essd-13-4349-2021.
Palmer, M.W., Earls, P.G., Hoagland, B.W., White, P.S., Wohlgemuth, T., 2002. Quantitative tools for perfecting species lists. Environmetrics 13, 121–137. https://doi.org/10.1002/env.516.
Pérez-Ramos, I.M., Álvarez-Méndez, A., Wald, K., Matías, L., Hidalgo-Galvez, M.D., Navarro-Fernández, C.M., 2021. Direct and indirect effects of global change on mycorrhizal associations of savanna plant communities. Oikos 130, 1370–1384. https://doi.org/10.1111/OIK.08451.
Qin, H., Lu, K., Strong, P.J., Xu, Q., Wu, Q., Xu, Z., Xu, J., Wang, H., 2015. Long-term fertilizer application effects on the soil, root arbuscular mycorrhizal fungi and community composition in rotation agriculture. Appl. Soil Ecol. 89, 35–43. https://doi.org/10.1016/J.APSOIL.2015.01.008.
Rocchini, D., Chiarucci, A., Oecologica, S.L.-A., 2004, undefined, 2004. Testing the spectral variation hypothesis by using satellite multispectral images. Elsevier. https://doi.org/10.1016/j.actao.2004.03.008.
Rondeaux, G., Steven, M., Baret, F., 1996. Optimization of soil-adjusted vegetation indices. Remote Sens. Environ. 55, 95–107. https://doi.org/10.1016/0034-4257(95)00186-7.
Rossi, C., Gholizadeh, H., 2023. Uncovering the hidden: leveraging sub-pixel spectral diversity to estimate plant diversity from space. Remote Sens. Environ. 296. https://doi.org/10.1016/j.rse.2023.113734.
Rouse, J., Haas, R., Schell, J., Publ, D.D.-N.S., 1974, Undefined, n.d. Monitoring Vegetation Systems in the Great Plains with ERTS. books.google.comJW Rouse, RH Haas, JA Schell, DW DeeringNASA spec. Publ, 1974•books.google.com.
Scheublin, T.R., Ridgway, K.P., Young, J.P.W., Van Der Heijden, M.G.A., 2004. Nonlegumes, legumes, and root nodules harbor different arbuscular mycorrhizal fungal communities. Appl. Environ. Microbiol. 70, 6240–6246. https://doi.org/10.1128/AEM.70.10.6240-6246.2004.
Schmid, M.W., van Moorsel, S.J., Hahl, T., De Luca, E., De Deyn, G.B., Wagg, C., Niklaus, P.A., Schmid, B., 2021. Effects of plant community history, soil legacy and plant diversity on soil microbial communities. J. Ecol. 109, 3007–3023. https://doi.org/10.1111/1365-2745.13714.
Schweiger, A.K., Cavender-Bares, J., Townsend, P.A., Hobbie, S.E., Madritch, M.D., Wang, R., Tilman, D., Gamon, J.A., 2018. Plant spectral diversity integrates functional and phylogenetic components of biodiversity and predicts ecosystem function. Nat. Ecol. Evol. 2, 976–982. https://doi.org/10.1038/s41559-018-0551-1.
Sexton, A.N., Conitz, F., Karlebowski, S., Neumann, A.E., Schmack, J.M., Sturm, U., Egerer, M., 2025a. Urban pollinator communities are structured by local-scale garden features, not landscape context. Landsc. Ecol. 403 (40), 50. https://doi.org/10.1007/s10980-025-02062-8.
Sexton, A.N., Conitz, F., Sturm, U., Egerer, M., 2025b. Wild plants drive biotic differentiation across urban gardens. Ecol. Evol. 15. https://doi.org/10.1002/ece3.71527.
Shannon, C.E., 1948. A mathematical theory of communication. Bell Syst. Tech. J. 27, 379–423. https://doi.org/10.1002/J.1538-7305.1948.TB01338.X.
Shipley, B., 2000. A new inferential test for path models based on directed acyclic graphs. Struct. Equ. Model. 7, 206–218. Doi: https://doi.org/10.1207/S15328007SEM0702_4;WGROUP:STRING:PUBLICATION.
Sørensen, M.B., Faurdal, D., Schiesaro, G., Jensen, E.D., Jensen, M.K., Clemmensen, L.K. H., 2025. Exploring crop health and its associations with fungal soil microbiome composition using machine learning applied to remote sensing data. Commun. Earth Environ. 61 (6), 355. https://doi.org/10.1038/s43247-025-02330-0.
Soudzilovskaia, N.A., van Bodegom, P.M., Terrer, C., Zelfde, M. van't, McCallum, I., Luke McCormack, M., Fisher, J.B., Brundrett, M.C., de Sá, N.C., Tedersoo, L., 2019. Global mycorrhizal plant distribution linked to terrestrial carbon stocks. Nat. Commun. 10, 1–10. https://doi.org/10.1038/S41467-019-13019-2;TECHMETA.
Soudzilovskaia, N.A., Vaessen, S., Barcelo, M., He, J., Rahimlou, S., Abarenkov, K., Brundrett, M.C., Gomes, S.I.F., Merckx, V., Tedersoo, L., 2020. FungalRoot: global online database of plant mycorrhizal associations. New Phytol. 227, 955–966. https://doi.org/10.1111/NPH.16569.
Sousa, D., Fisher, J.B., Galvan, F.R., Pavlick, R.P., Cordell, S., Giambelluca, T.W., Giardina, C.P., Gilbert, G.S., Imran-Narahari, F., Litton, C.M., Lutz, J.A., North, M.P., Orwig, D.A., Ostertag, R., Sack, L., Phillips, R.P., 2021. Tree canopies reflect mycorrhizal composition. Geophys. Res. Lett. 48. https://doi.org/10.1029/2021GL092764.
Stahlhut, K.N., Neupert, D.G., Laing, J.E., Witt, L.J., Bauer, J.T., 2024. Measuring leaf and root functional traits uncovers multidimensionality of plant responses to arbuscular mycorrhizal fungi. Am. J. Bot. 111. https://doi.org/10.1002/AJB2.16369.
Sun, Z., Song, J., Xin, X., Xie, X., Zhao, B., 2018. Arbuscular mycorrhizal fungal 14-3-3 proteins are involved in arbuscule formation and responses to abiotic stresses during AM symbiosis. Front. Microbiol. 9, 311904. https://doi.org/10.3389/FMICB.2018.00091/BIBTEX.
Taddeo, S., Dronova, I., Harris, K., 2021. Greenness, texture, and spatial relationships predict floristic diversity across wetlands of the conterminous United States. ISPRS J. Photogramm. Remote Sens. 175, 236–246. https://doi.org/10.1016/j.isprsjprs.2021.03.012.
Tibshirani, R., 1996. Regression shrinkage and selection via the Lasso. J. Royal Statistical Soc. Series B: Statistical Methodol. 58, 267–288. https://doi.org/10.1111/J.2517-6161.1996.TB02080.X.
Valbuena, R., Packalén, P., Martín-Fernández, S., Maltamo, M., 2012. Diversity and equitability ordering profiles applied to study forest structure. For. Ecol. Manag. 276, 185–195. https://doi.org/10.1016/J.FORECO.2012.03.036.
Vályi, K., Rillig, M.C., Hempel, S., 2015. Land-use intensity and host plant identity interactively shape communities of arbuscular mycorrhizal fungi in roots of grassland plants. New Phytol. 205, 1577–1586. https://doi.org/10.1111/NPH.13236.
Van Cleemput, E., Vanierschot, L., Fernández-Castilla, B., Honnay, O., Somers, B., 2018. The functional characterization of grass- and shrubland ecosystems using hyperspectral remote sensing: trends, accuracy and moderating variables. Remote Sens. Environ. 209, 747–763. https://doi.org/10.1016/J.RSE.2018.02.030.
Van Der Heijden, M.G.A., Klironomos, J.N., Ursic, M., Moutoglis, P., Streitwolf-Engel, R., Boller, T., Wiemken, A., Sanders, I.R., 1998. Mycorrhizal fungal diversity determines plant biodiversity, ecosystem variability and productivity. Nature 396, 69–72. https://doi.org/10.1038/23932;KWRD.
Van Nuland, M.E., Averill, C., Stewart, J.D., Prylutskyi, O., Corrales, A., van Galen, L.G., Manley, B.F., Qin, C., Lauber, T., Mikryukov, V., Dulia, O., Furci, G., Marín, C., Sheldrake, M., Weedon, J.T., Peay, K.G., Cornwallis, C.K., Větrovský, T., Kohout, P.,

Baldrian, P., Tedersoo, L., West, S.A., Crowther, T.W., Kiers, E.T., van den Hoogen, J., 2025. Global hotspots of mycorrhizal fungal richness are poorly protected. Nat 6458080 (645), 414–422. https://doi.org/10.1038/s41586-025-09277-4.

Wang, R., Gamon, J.A., 2019. Remote sensing of terrestrial plant biodiversity. Remote Sens. Environ. 231, 111218. https://doi.org/10.1016/J.RSE.2019.111218.

Wang, R., Gamon, J.A., Emmerton, C.A., Li, H., Nestola, E., Pastorello, G.Z., Menzer, O., 2016. Integrated analysis of productivity and biodiversity in a southern Alberta prairie. Remote Sens. 8, 1–20. https://doi.org/10.3390/rs8030214.

Wang, M., Wang, Z., Guo, M., Qu, L., Biere, A., 2023. Effects of arbuscular mycorrhizal fungi on plant growth and herbivore infestation depend on availability of soil water and nutrients. Front. Plant Sci. 14, 1101932. https://doi.org/10.3389/FPLS.2023.1101932/BIBTEX.

Xiao, D., Che, R., Liu, X., Tan, Y., Yang, R., Zhang, W., He, X., Xu, Z., Wang, K., 2019. Arbuscular mycorrhizal fungi abundance was sensitive to nitrogen addition but diversity was sensitive to phosphorus addition in karst ecosystems. Biol. Fertil. Soils 555 (55), 457–469. https://doi.org/10.1007/s00374-019-01362-x.

Xie, T., Lin, Y., Li, X., 2024. Responses of the arbuscular mycorrhizal fungi community to warming coupled with increased drought in an arid desert region. Geoderma 441, 116744. https://doi.org/10.1016/J.GEODERMA.2023.116744.

Zhou, Y., Chen, K., Muneer, M.A., Li, C., Shi, H., Tang, Y., Zhang, J., Ji, B., 2022. Soil moisture and pH differentially drive arbuscular mycorrhizal fungal composition in the riparian zone along an alpine river of Nam co watershed. Front. Microbiol. 13, 994918. https://doi.org/10.3389/FMICB.2022.994918/FULL.